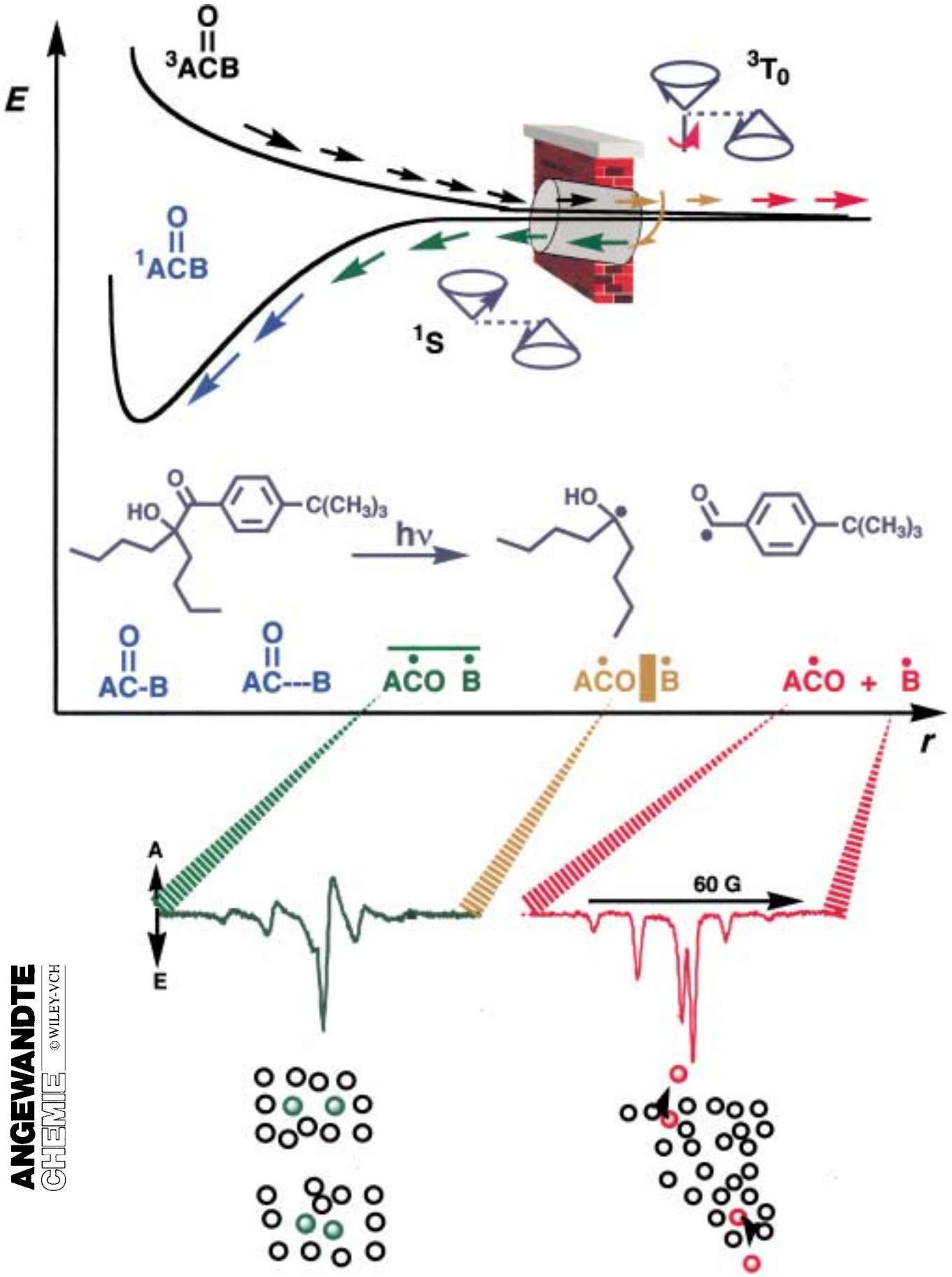

Detailed monitoring of the photochemical *α*-cleavage of ketones is possible with the TREPR technique.

Electron Spin Polarization and Time-Resolved Electron Paramagnetic Resonance: Applications to the Paradigms of Molecular and Supramolecular Photochemistry

Nicholas J. Turro,* Mark H. Kleinman, and Erdem Karatekin

Most molecular and supramolecular organic photochemical reactions involve paramagnetic reactive intermediates (such as molecular triplet states, triplet radical pairs, and free radicals). In a number of cases these species are created with "anomalous" spin populations which are far from thermal equilibrium. Such paramagnetic species are said to be "spin polarized" and may be observed directly by time-resolved electron paramagnetic resonance (TREPR). The TREPR technique can be applied to exploit spin polarization, which, in addition to providing an enormous signal to noise enhancement, also reveals the mechanisms involved in photochemical reactions. TREPR spectroscopy provides a means of tracking the reaction of radicals with molecules and the nonreactive interactions of radicals with other radicals in real time. The latter interactions provide a systematic investigation of supramolecular interactions of geminate radicals in micelles.

Keywords: EPR spectroscopy · paradigms · photochemistry · radicals · supramolecular chemistry

1. Paradigms, Electron Polarization, Time-Resolved Electron Paramagnetic Resonance, and Photochemistry

This review attempts to tie together the paradigms of several fields: organic photochemistry, time-resolved electron paramagnetic resonance (TREPR), electron spin polarization (ESP), and supramolecular chemistry. A major goal of the authors is to provide organic chemists and physical organic chemists with a nonmathematical overview and appreciation of how TREPR and ESP can contribute to an understanding of the paramagnetic species (triplet states, radical pairs, and radicals) which are commonly produced in organic photoreactions. Although the approach is qualitative and exemplary, the interested reader is referred to any one of a number of excellent quantitative reviews on TREPR and ESP which have appeared.[1–7]

This review presents a general working paradigm for organic photochemistry which can be examined by the TREPR technique and for which ESP plays a major role in providing both mechanistic, structural, and dynamic information on the paramagnetic intermediates involved in photochemical reactions. After a brief qualitative and conceptual review of EPR emphasizing the importance of the simpler aspects of transitions between magnetic energy levels, the phenomenon of ESP and its impact on TREPR spectroscopy is described. With this background the reader is provided with an exemplar photochemical reaction, the α-cleavage of carbonyl compounds, which is examined in detail by first using magnetic energy level diagrams to predict the attributes expected from TREPR spectra. These expectations are then compared to experimental examples of TREPR spectroscopy of the paramagnetic intermediates involved in the photochemical α-cleavage of carbonyl compounds. Examples are then given of 1) the creation of ESP by intersystem crossing from excited singlet states of carbonyl compounds; 2) the creation of ESP by the primary photochemical reactions of spin-polarized molecular triplets; 3) the transfer of ESP by reaction of polarized radicals with molecular scavengers; 4) the transfer of ESP by nonreactive collisions between radicals; and 5) the sorting of ESP by nonreactive collisions between radicals. The account concludes with a description of how TREPR can be employed to examine supramolecular structure and dynamics of geminate radical pairs adsorbed in micelles.

[*] Prof. Dr. N. J. Turro, M. H. Kleinman, E. Karatekin
Department of Chemistry
University of Columbia
Havemeyer Hall, New York, NY 10027 (USA)
Fax: (+1) 212-932-1289
E-mail: turro@chem.columbia.edu

1.1. Paradigmatic Science and Paradigmatic Chemistry

According to Kuhn,[8] ordinary scientific research is executed under the implicit control of *paradigms*. The term

  1433-7851/00/3924-4437 $ 17.50+.50/0

"paradigm" is often used loosely in several different contexts: 1) There are *global paradigms* referring to an entire constellation of beliefs, values, techniques, methods, etc. that are shared by the practitioners of a given scientific discipline. To a large extent the nature of a scientific discipline is determined by the shared global paradigms, which achieve their authority over the practitioners from the sociological and community-based structure of a science. 2) There are also everyday *working paradigms* which are based on experience with specific areas of normal, everyday research and which tend to be generally and broadly applicable when investigating systems having some precedent; 3) Finally there are *exemplar paradigms* or specific concrete examples, widely considered by the community to be outstanding research accomplishments, which serve as models for previous, current, and future research by practitioners.

1.2. The Paradigm of Molecular Organic Photochemistry

The global, working, and exemplar paradigms of molecular organic photochemistry determine the everyday "normal science" activities of organic photochemists by defining entities and transitions between entities that are generally involved in typical organic photochemical reactions.[9] Let us consider the development of these three paradigms defining the entities and transitions that are essential for organic photochemical reactions involving a transformation from a reactant R to a product P. A very condensed representation of the global paradigm is found in Scheme 1. In words, the global paradigm states that an organic photochemical reaction generally proceeds as follows: the absorption of a photon by R produces an electronically excited state *R that undergoes primary photochemical reactive transitions to form a reactive intermediate I. At this point the photochemistry has ended.

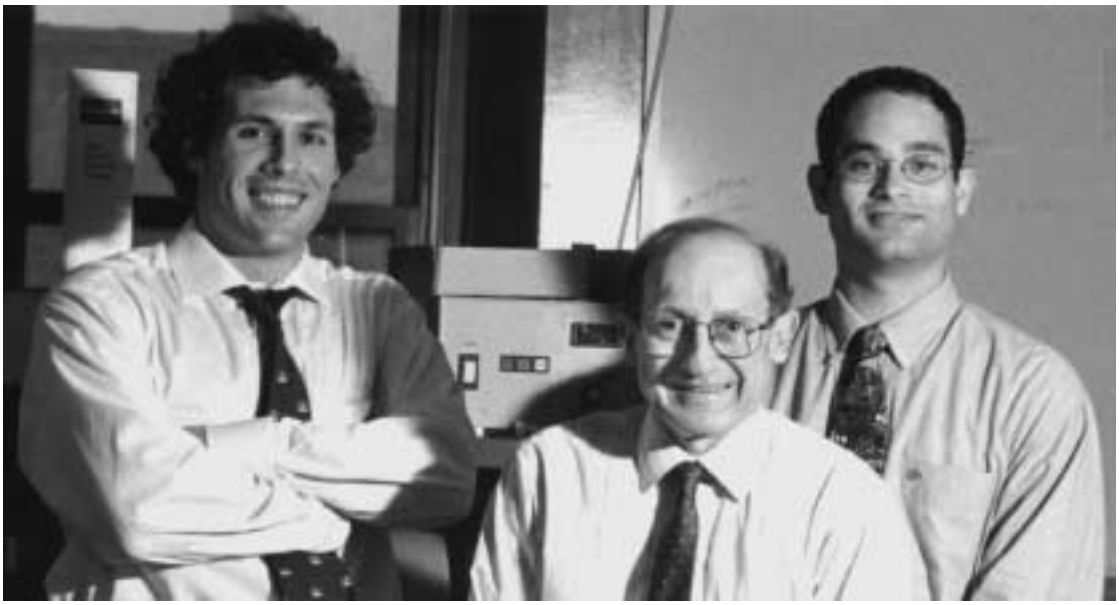

E. Karatekin N. J. Turro M. H. Kleinman

Nicholas J. Turro was born in Middletown (Connecticut, USA), in 1938. He received his Ph.D. degree from Caltech in 1963 and joined the faculty at Columbia University in 1964, where he is currently the William Schweitzer Professor of Chemistry. His research interests include the use of photochemistry and spectroscopy to investigate the structure and dynamics of molecular and supramolecular systems.

Mark H. Kleinman was born in Montreal (Québec, Canada) in 1969. Heading westward, he worked with C. Bohne at the University of Victoria (British Columbia, Canada) where he studied the dynamics of radicals in supramolecular systems and received his Ph.D. in 1998. He is currently working with N. J. Turro, G. W. Flynn, and P. Schlosser as a Dreyfus postdoctoral fellow at Columbia University. His main research interests include triplet state mediated photochemistry and the application of spectroscopic techniques to investigate dynamic processes in biological and environmental systems.

Erdem Karatekin was born in Ankara (Turkey) in 1972. He received his B.S. degree in chemical engineering from the University of Louisville, Kentucky. He has recently completed his Ph.D. degree under the mentorship of N. J. Turro and B. O'Shaughnessy at Columbia University, where his research focused on the use of photochemical techniques in the study of free radical polymerization and polymer reaction kinetics. After leaving Columbia he joined the Institut Curie in Paris for a post-doctoral position with F. Brochard and J. L. Viovy.

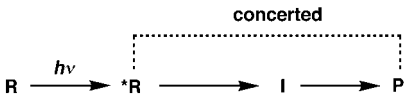

Scheme 1. Schematic representation of a global paradigm for molecular organic photochemistry. Concerted reactions (dashed line) are rare in photochemical reactions.

The reactive intermediate I then proceeds through secondary ordinary thermal processes to the isolated product P. Simply put, the photochemist will start an analysis of a photoreaction $R+h\nu \rightarrow P$ by considering the entities and transitions involved in the pathways shown in Scheme 1 and then proceed with the analysis by including all of the explicit and implicit knowledge that is "globally" accepted by the photochemical community.

1.2.1. A Working Paradigm for Organic Photochemistry

The global paradigm of Scheme 1 may be expanded and elaborated into a general working paradigm for the photoreactions of families of organic molecules. For any family of molecules the working paradigm usually considers orbital and spin descriptions (configurations) of the entities (R, *R, I, and P) shown in Scheme 1. It is usually sufficient to start by classifying *R and I according to the orbital nature and spin orientation of the electrons in the singly occupied (SOMO), highest occupied ground state orbital (HOMO), and lowest unoccupied ground state orbital (LUMO) as shown in Scheme 2, which represents a working paradigm for the

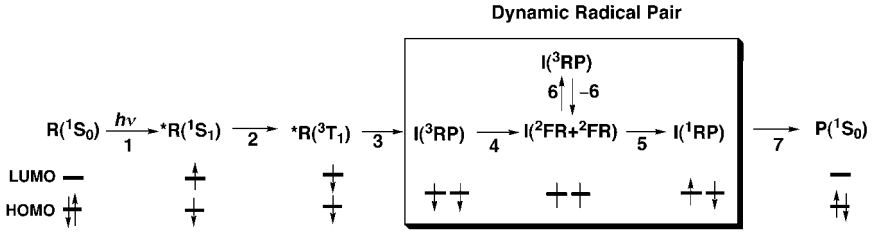

Scheme 2. A working paradigm for the photochemistry of organic molecules, in particular, for the photochemistry of ketones. The arrows are schematic representations of electronic spins. In the case of the electronic spins indicated for $I(^2FR)$, the lines represent spins that have orientation but do not interact with each other. See text for a description of mechanistic steps.

molecular photochemistry of ketones (AC(O)B), the family of molecules that are of greatest interest in this account. In the working paradigm the structures of the generalized concept of excited states and reactive intermediates are amplified to include the orbital and spin structures of *R and I. In addition, certain details of the dynamic behavior of intermediates that have been shown to be commonly important, such as the dynamic behavior of radical pairs and free radicals (box in Scheme 2), are included. Throughout this account much of what is written about radical pairs will be analogous to the chemistry of biradicals,[2, 10, 11] which are beyond the scope of this review.

In Scheme 2, the superscripts 1, 2, and 3 are employed to denote the spin multiplicities of the entities. These terms and the spin features will be explained in more detail in Section 1.3.3. Both starting material and products are ground-state singlet states, $R(^1S_0)$ and $P(^1S_0)$, and possess an electronic configuration with two electrons in the HOMO (and all lower energy orbitals) and no electrons in the LUMO. *R may be either a singlet $*R(^1S_1)$ or a triplet $*R(^3T_1)$ species, where both possess one electron in the HOMO and one electron in the LUMO. Similarly, I may be either a singlet $I(^1RP)$ or a triplet $I(^3RP)$ species, but in this case each possesses one electron in separate SOMOs. Depending on the ketone structure, each of these entities may be assigned an electronic orbital configuration (for example, n,π*, π,π*). In the photochemistry of ketones, the intermediate I actually represents interrelated groups of entities that can be termed "dynamic radical pairs" (RP) and "free radicals" (FR, box in Scheme 2). The concept of the dynamic radical pair is essential for an understanding of organic molecular and supramolecular photochemistry and will be discussed at several junctures in this account.

Based on a wide range of experience, a photochemist is likely to accept Scheme 2 as an initial working paradigm for investigating and analyzing the photochemistry of ketones. Thus, a photoreaction of a ketone is generally assumed to involve the following connected transformations: the absorption of a photon by $R(^1S_0)$ produces an electronically excited singlet state $*R(^1S_1)$ (step 1) which undergoes an efficient conversion into an electronically excited triplet state $*R(^3T_1)$ through a transition termed intersystem crossing (ISC, step 2). In this step, spin is apparently created as $*R(^1S_1)$ and has a net spin of zero, but $*R(^3T_1)$ has a net spin of one. $*R(^3T_1)$ is usually the electronically excited entity responsible for the photochemistry of ketones, that is, $*R(^3T_1)$ undergoes the primary photochemical reaction (step 3).

Implicit in the global paradigm of photochemistry is the notion that all primary photochemical processes are elementary steps and that all elementary steps obey spin conservation laws (total spin is conserved in an elementary reaction). Thus the primary photochemical reaction (step 3) from $*R(^1T_1)$ produces a geminate triplet radical pair $I(^3RP)$. The dynamic radical pair must operate under spin selection rules, that is, $I(^3RP)$ cannot undergo elementary radical–radical reactions to form singlet molecules such as $P(^1S_0)$, since such an elementary step would violate spin selection rules. As a result, the geminate triplet pair separates (step 4) to produce two free radicals $I(^2FR+^2FR)$. In spin terminology, each free radical is termed a doublet and labeled with a superscript 2. The ^2FRs undergo diffusion excursions (see Section 3.1.1) and are considered to be part of the dynamic radical pair system indicated in Scheme 2. In the absence of scavengers (which are left out at this point for the sake of simplicity) two ^2FR's, after certain diffusional excursions in solution, will eventually encounter to produce random singlet radical pairs $I(^1RP)$ (step 5) or triplet radical pairs $I(^3RP)$ (step 6) in the ratio of 1:3 (based on spin statistics). According to the working paradigm the isolated products (P) may only form from the radical–radical reactions of the singlet radical pairs $I(^1RP)$ (step 7). The random triplet radical pairs $I(^3RP)$ separate again into $I(^2FR)_2$

(step −6), and continue to cycle through steps −6, 6, and 7 until the reaction is complete and all the radicals are consumed. The radical–radical reactions or RP are conventionally termed "combination reactions" which applies to reactions in which the pair actually combine by bond formation to form a molecule, or undergo disproportionation to form two molecules.

In most actual photochemical reactions each entity on the pathway from R to $P(^1S_0)$ will also have other options that are not shown in Scheme 2. The chemical and quantum yield of formation of $P(^1S_0)$ depends on how these options compete with those on the pathway from R to $P(^1S_0)$. Since these options are well known to the photochemist through the global paradigm, they are not explicitly included in the working paradigm. For example, in addition to the radical–radical reactions shown in the example, $*R(^3T_1)$ may undergo more than one primary photochemical process in step 3 to form other products $P_i(^1S_0)$. One of the primary ^2FR formed in step 4 may undergo radical–radical transformations (unimolecular rearrangements or fragmentations) or undergo reactions with scavengers to form secondary free radicals $(^2FR)_2$, that eventually undergo radical–radical reactions to form other products $P_i(^1S_0)$. The working paradigm of Scheme 2 (and the implicit options that are designated by the global paradigm) works extremely well for the molecular photochemistry of ketones in nonviscous homogeneous solutions for which the separation of the triplet radical pair into ^2FR is very efficient. We shall see in Section 3.1 that the working paradigm of Scheme 2 can be readily adapted to accommodate supramolecular systems.

1.2.2. Electron Spin Polarization and TREPR

This review is concerned with the phenomenon of electron spin polarization (ESP) and the TREPR technique, which takes great advantage of ESP. The combination of ESP and TREPR provides the power to directly or indirectly observe *all* of the paramagnetic entities listed in Scheme 2 ($^3T_1$, ^3RP, ^2FR) and to elucidate the connecting transitions leading to or from these species (for example, $^1S_1 \rightarrow {}^3T_1$, $^3T_1 \rightarrow {}^2FR + {}^2FR$, transformations of the dynamic radical pair, $RP \rightarrow {}^2FR'$). In addition, we shall see how ESP and TREPR provide a means of elucidating "invisible" intermolecular (supramolecular) interactions, such as nonreactive intermolecular collisions between paramagnetic species, that are implicit in the working paradigm (for example, $^2FR + {}^2FR \rightarrow {}^3RP$). A further remarkable feature of the TREPR technique is that, in addition to information that will confirm that these elementary steps have occurred, TREPR will reveal some very subtle and somewhat esoteric features of these transitions. For example, the spin sublevel selectivity of each of these reactive and nonreactive transitions can be investigated. Finally, we shall see that ESP is a common feature of the elementary steps involving the paramagnetic entities in Scheme 2 and that ESP serves to enhance the signal-to-noise ratio of the TREPR method and acts as a nonintrusive label of paramagnetic species.

Since TREPR deals with the investigation of photochemical reactions in an applied magnetic field, we will now consider how the molecular photochemistry paradigm must be modified as the result of the presence of a magnetic field and develop a paradigm as to how electron spin polarization is created, sorted, and transferred.

1.3. Electrons In a Strong Applied Magnetic Field—EPR Spectroscopy

Investigation of photochemical reactions by EPR involves the study of photochemistry in a magnetic field. Thus, a photochemist needs to modify the working paradigm by including the effects of an applied magnetic field on the entities and transitions in Scheme 2. It is expected that all of the paramagnetic entities ($^3T_1$, ^3RP, and ^2FR) and transitions involving these paramagnetic species will be influenced by the presence of a strong applied magnetic field. Since they are diamagnetic, the singlet entities $^1R(S_0)$, $^1*R(S_1)$, $I(^1RP)$, and $^1P(S_0)$ are not expected to be influenced by the applied magnetic field.

In this section we provide a qualitative and elementary description of the behavior of the paramagnetic entities and how their transitions are influenced by a strong magnetic field. This description is intended to provide the reader with a feeling of how TREPR may serve as a powerful tool to elucidate the structure and transformations of the entities of the working paradigm for photochemistry. An apology is in order at this point to experts who may be concerned with the level of simplification. The simplification is intended to capture the essential qualitative features of very complex phenomena and follow through with the consequence of a set of rules that can be visualized on a simplified model. The article is intended for the organic chemist who has had little or no detailed experience with EPR. References are given throughout to more detailed and advanced discussions.

1.3.1. The Simplest Case: EPR of a Free Electron

EPR spectroscopy involves the experimental observation of transitions between magnetic sublevels in a magnetic field. Thus, for a qualitative understanding of EPR we need to understand how the sublevels of the paramagnetic entities in Scheme 2 are influenced by the application of a strong applied magnetic field. We shall consider only three simple cases: 1) a single electron; 2) a single electron interacting with a spin ½ nucleus; and 3) two interacting electrons. These cases will serve as a basis for understanding the features of EPR, TREPR, and ESP of all of the paramagnetic entities of Scheme 2.

For the simplest case we consider the effect of an applied external magnetic field (B_0) on a single isolated, "free" electron which does not interact with any other electron spins or nuclear spins.[12, 13] The spin of an electron S is associated with a magnetic moment μ, and both are vector quantities. When placed in a magnetic field, the electron spin is required by quantum mechanics to assume definite orientations with respect to the direction of the external magnetic field. The energy separating the magnetic energy levels of this electron depends linearly on the strength of the external magnetic field (Scheme 3). The magnetic interaction which causes this

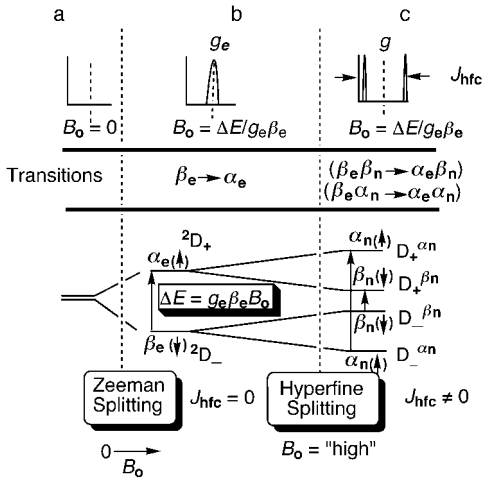

Scheme 3. Energy level diagram describing the origin of EPR spectra of a single electron and an electron coupled to a spin ½ nucleus. Top: Observed EPR spectra derived from electronic transitions; bottom: energy level diagram depicting the transitions in the absence (case a, $B = 0$), "low" levels (case b, Zeeman splitting), and high levels (case c) of an applied magnetic field. For clarity, the energy levels split by hyperfine coupling in case c are pictured with larger energy gaps. See text for a full description.

energy difference is termed the Zeeman interaction, and is given by Equation (1). β_e is the Bohr magneton ($\beta_e = 9.27 \times 10^{-24}\,J\,T^{-1}$) and g_e is the free electron "g-factor", a unitless

$$\Delta E_{Zeeman} = g_e\beta_eB_o \quad (1)$$

value which is equal to 2.0023. From Equation (1) it is seen that the energy gap between two magnetic levels is proportional to the magnitude of the applied field B_0, and the g-factor. The latter is analogous to the chemical shift of NMR spectroscopy. It is important to note that the spin angular momentum difference between the two adjacent magnetic sublevels is always exactly one unit of spin angular momentum, but the energy difference depends on the strength of the applied field and the g-factor of the radical.

When the angular momentum of an electron is aligned parallel to an applied magnetic field (the magnetic moment vector points in the same direction as the field), its magnetic energy is higher than when the angular momentum is aligned antiparallel to it. The higher energy spin orientation is termed an "up" spin (↑) or an α spin and will be noted as $\alpha(\uparrow)$. The lower energy spin is termed a "down" spin (↓) or a β spin and will be noted as $\beta(\downarrow)$. The effect of an applied magnetic field is to break the degeneracy of the two orientations in energy, with the $\beta(\downarrow)$ level dropping and the $\alpha(\uparrow)$ rising as the field strength increases [Eq. (1)].

In practice, an orbitally unpaired electron is bound to one or more nuclei, such as an unpaired electron in a carbon-centered free radical. This situation causes two effects: 1) the g-factor of the radical, which determines the strength of the Zeeman interaction and the energy gap in Equation (1), will differ from that of the free electron, g_e, and 2) the unpaired electron will interact or "couple" with the magnetic moments of the neighboring nuclei that make up the radical, to produce the so-called "hyperfine coupling" (hfc) of electron spins to nuclear spins (which is analogous to the spin–spin coupling of nuclear spins). Typical g-factors for organic radicals range between 2.010 and 1.990 (compared to a value of 2.0023 for the free electron). Although these differences in g-factors are small, they can be measured with sufficiently high precision, so that g-factors (like chemical nuclear shifts in NMR) provide valuable information on the structure of a given radical.[14]

Conventional commercial EPR spectrometers operate at a single frequency, usually between 9 and 10 GHz, so that the EPR transitions for a free electron measured in Equation (1) will occur at magnetic fields of the order of 3500 gauss (3500 G or 0.35 T). The EPR spectrum of a free electron will consist of a single "line" (Scheme 3b), which results form the absorption of a photon whose frequency corresponds to the energy of $g_e\beta_eB_0$ [Eq. (1)]. The photon induces the transitions of electron spins from the more heavily populated $\beta(\downarrow)$ orientation to the $\alpha(\uparrow)$ orientation (and from the lesser populated $\alpha(\uparrow)$ to $\beta(\downarrow)$). This change in orientation, in turn, corresponds to a change in spin of one unit of spin angular momentum ($-\frac{1}{2} \rightarrow +\frac{1}{2}$), which is exactly the spin angular momentum possessed by a photon. The conservation of spin angular momentum in the absorption of electromagnetic radiation serves as the basis for first order selection rules for EPR transitions. Thus, the $\beta \rightarrow \alpha$ transition is said to be EPR "allowed" to a first approximation, as is the reverse transition $\alpha \rightarrow \beta$. Thus, the selection rule to the first approximation is very simple: a radiative EPR transition (absorption or emission) is allowed when the electron flips its orientation from $\beta \rightarrow \alpha$ or $\alpha \rightarrow \beta$. As will be discussed in Section 1.4, the intensity of the absorption will depend on the difference in populations between the spins in the β and α orientations.

1.3.2. EPR Spectrum of an Electron Coupled to a Nucleus of Spin ½

The energy levels for a free electron placed in a magnetic field and the manner in which the levels are modified by the presence of a neighboring nucleus of spin ½ (for example, a proton or a ^{13}C nucleus) are shown in Scheme 3c. The EPR spectrum of a hydrogen atom, the simplest free radical (an electron and a proton) provides a model for the effects of the hyperfine coupling of an unpaired electron and a spin ½ nucleus. The nuclear spin states (α_n or β_n) are shown on the energy levels. (The energy levels are not drawn to scale and the actual ranking of energy levels depends on several factors, such as the sign of the hyperfine coupling constants.) As for the free electron, only the $\beta_e \rightarrow \alpha_e$ EPR absorptive transitions are allowed (arrow in Scheme 3b). In addition, a second selection rule now applies: the nuclear spin cannot change its orientation from α to β or β to α during the electronic spin transition. This rule may be considered as the spin analogue of the Franck–Condon Principle for electronic transitions, and denotes that electron spin reorientation caused by the absorption of a photon occurs much more rapidly than the reorientation of a nuclear spin. Thus, the spin orientation immediately before and after the electron spin flip is the same.

From the spin selection rules, only two EPR transitions are allowed for β_e (arrows in Scheme 3c): $\beta_e\beta_n \rightarrow \alpha_e\beta_n$ and $\beta_e\alpha_n \rightarrow \alpha_e\alpha_n$. From the scheme it is seen that the energies

and therefore the frequencies of these transitions are clearly different so that two lines appear in the EPR spectrum. Working through the paradigm of hyperfine coupling, the two lines are split an equal amount about the position defined by the *g*-factor of the radical. The separation between the lines is equal to the hyperfine coupling constant J_{hfc}. Note that by convention in EPR spectroscopy, the hfc constant is represented as an "*a*", however, since more readers are familiar with NMR spectrosocopy, here we use "NMR-type" nomenclature *J*. Coupling with more than one spin causes the number of energy levels to increase, and the mixing of levels requires higher order considerations; but in general, Scheme 3 captures the essence of the qualitative information that is needed to obtain an appreciation of the origin of the EPR effects of interest in this account.

It should be pointed out that the higher the energy of an EPR transition, the lower the field at which the transition occurs at a fixed frequency. Thus the transition for which the α nucleus is involved occurs at lower field than the transition for which the β transition occurs (Scheme 3). From Equation (1) it can be deduced that the larger the *g*-factor, the lower the center field for a hyperfine pattern.

1.3.3. Paramagnetic Species in a Magnetic Field—Singlet (^{1}S), Doublet (^{2}D), and Triplet (^{3}T) States

We are now in a position to discuss the total spin labels of the entities of Scheme 2 and how these labels can be used in magnetic energy level diagrams. The entities with superscript 1 possess a total spin of zero in any orientation in a magnetic field and are termed singlet (^{1}S) states (for example, R($^1S_0$), R($^1S_1$), (^{1}RP) and P($^1S_0$)). For *R and I, singlet states result when two orbitally unpaired electrons have an α and β orientation and interact to yield a net spin of 0. Singlets are diamagnetic (nonmagnetic) and their energies are not affected by an applied magnetic field. This means that the energy level of a given singlet state remains a single level in a magnetic field and that there is no Zeeman effect of magnetic state.

The free radical entities of Scheme 2 are described by a superscript 2 and possess a total spin of ½ in the orientation of the spin and are termed doublet (^{2}D) free radical states (^{2}FR (^{2}D)). Doublets are paramagnetic and their energies are influenced, as described in Sections 1.3.1 and 1.3.2, by an applied field which splits doublet species into the two states $^2D_+(\alpha)\uparrow$ and $^2D_-(\beta)\downarrow$. The subscripts + and − are derived from the fact that the $\alpha(\uparrow)$ state has a spin angular momentum of $+½$ on the magnetic field axis and the $\beta(\downarrow)$ state has spin angular momentum of $-½$ on the magnetic field axis.

Let us now consider the energy diagram that results when two orbitally unpaired electrons (or more generally, two spin ½ particles) interact to create a total spin of 1. In a spin 1 state there are three possible orientations of the spin in a strong magnetic field. These three states are termed $^3T_+$, $^3T_0$, and $^3T_-$. In the absence of the applied field, the three levels have the same energy (except for a small "zero field" energy arising from electron–electron spin interactions). As the field is applied, the Zeeman interaction splits the energies of the triplet in a manner that depends upon the orientation of the total spin relative to the applied field. The subscripts +, 0, and − correspond to the magnitude of the spin angular momentum on the magnetic field axis of +1, 0, and −1. The $^3T_+$ state, which possesses two $\alpha(\uparrow)$ spins increases in energy and the $^3T_-$ state, which possesses two $\beta(\downarrow)$ spins, decreases in energy as the field strength increases. The energy separation is given by an expression analogous to Equation (1), except that the *g*-factor refers to the triplet state and the total spin must be taken into account. Scheme 4a shows schematically the magnetic energy sublevel diagram for the interconversion of $^3T_1 \rightarrow {}^3RP \rightarrow {}^2FR + {}^2FR$. The energy diagrams of $^3T_1$ and ^{3}RP are expected to be similar, since both involve spin-correlated

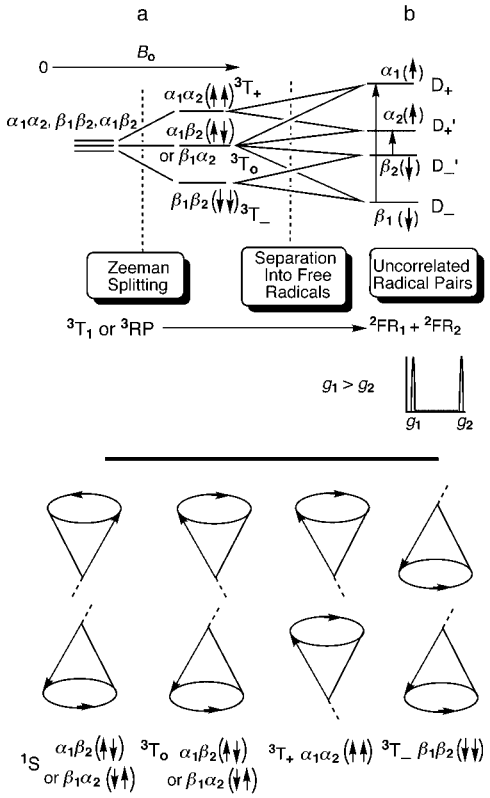

Scheme 4. Top: Spin-correlation diagram for a triplet state which undergoes a primary photochemical process to produce a pair of free radicals. a) Represents the energy diagram for triplet species (^{3}T or ^{3}RP), while case b) is the energy diagram for two free radicals $^2FR_1$ and $^2FR_2$. It is assumed that $^2FR_1$ has a larger *g*-factor than $^2FR_2$. The energies are not to scale. Bottom: spin vectors for the singlet and three triplet states. See text for more discussion.

pairs. In homogeneous fluid solution ^{3}RP is generally not detectable as an intermediate because of the very short lifetime of the pair in nonviscous solvents. However, we shall see that in supramolecular systems the lifetime of ^{3}RP may be extended considerably so that spin-correlated radical pairs can be observed directly by the TREPR technique. We shall make use of the correlation diagram of Scheme 4 when discussing the triplet mechanism for producing ESP in the α-cleavage reactions of ketones in Section 2.3.2.

Both a singlet state ^1S and the $^3T_0$ state possess one $\alpha(\uparrow)$ spin and one $\beta(\downarrow)$ spin. As shown in Scheme 4, the root of the difference between the triplet and singlet states is the relative phase of the spin vectors. The spin vectors for the ^1S state are oriented so as to completely cancel the individual angular momentum and lead to a net spin of zero (antiparallel orientations with respect to the field, 180° out of phase), whereas the spin vectors of $^3T_0$ are oriented so that the total angular momentum adds to one (antiparallel with respect to the field, in phase). $^3T_0$, which possesses one $\alpha(\uparrow)$ spin and one $\beta(\downarrow)$ spin, does not change in energy as the field is applied, because it does not possess a net magnetic moment in the direction of the field (the direction of the total spin is perpendicular to the magnetic field axis). A handy representation of the spin orientation of the three triplet sublevels is $^3T_+[\alpha,\alpha(\uparrow\uparrow)]$, $^3T_0$ [either $\alpha\beta(\uparrow\downarrow)$ or $\beta\alpha(\downarrow\uparrow)$], and $^3T_-$ $[\beta\beta(\downarrow\downarrow)]$. However, although this notation is appropriate for the $^3T_+$ and $^3T_-$ states, the $^3T_0$ state is not properly represented by this notation because it does not properly define the phase of the spins. Indeed, in this representation the singlet state and $^3T_0$ state are not distinguished. This issue will be dealt with in Section 2.2.1 where spin correlation and singlet–triplet interconversion are considered.

The vector representation in Scheme 4) provides a handy shorthand and guide for the spin-correlation diagram to connect the processes $^3T_1 \rightarrow {}^3RP \rightarrow {}^2FR + {}^2FR$, which are of key importance in the photochemical paradigm of Scheme 2. In this notation the singlet state which correlates with the ^2FR is represented as ^1S[either $\alpha\beta(\uparrow\downarrow)$ or $\beta\alpha(\downarrow\uparrow)$]. As discussed above for $^3T_0$, this notation needs to be modified, since at this level, S and T_0 are indistinguishable. Similar to $^3T_0$, the energy of ^1S is not affected by the application of an applied field, because it does not possess a net magnetic moment in any direction and therefore doesn't interact with the field. However, the energy gap between $^3T_0$ and ^1S depends on the distance of separation of the electrons possessing the unpaired spins. In the molecular triplet, the electrons are held close to one another by the molecular framework (Scheme 4a). This proximity leads to a large J value, the electron exchange interaction, which is the basis of the singlet–triplet energy difference. As the system proceeds from $^3T_1 \rightarrow {}^3RP \rightarrow {}^2FR + {}^2FR$, the electrons and their associated spins get further and further apart and the energy gap between $^3T_0$ and ^1S decreases toward a value of zero. When the system forms a pair of free radicals ($^2FR + {}^2FR$), the value of J is zero and the system has lost the correlated magnetic characteristics of a spin one system (a triplet, $^3T_1$) and has taken on the magnetic characteristics of two uncorrelated spin ½ systems ($^2D_1$, $^2D_1$, two doublets).

The EPR spectrum of doublets has been discussed above in simple terms (see Scheme 3b). The EPR spectrum of a molecular triplet is very complicated because of the strong spin–spin interactions of the two spins which are tightly coupled together by the molecular framework and the fact that the energy gap between triplet sublevels depends on the orientation of the triplet molecule in the magnetic field. We shall postpone a discussion of the EPR spectrum of $^3T_1$ and ^3RP until actual examples are presented in Section 2.3. However, formation of ^3RP from $^3T_1$ greatly reduces the spin–spin interactions and in some circumstances, the EPR spectrum may be considered in terms of two interacting doublets (as will be discussed in Section 3.3).

1.4. Electron Spin Polarization (ESP)

An important characteristic of TREPR spectra is the common observation that EPR signals often occur at the same frequencies as in conventional steady-state EPR spectra, but the signals have "anomalous" intensities of "enhanced absorption" (A) or may actually appear in "emission" (E). Since the frequencies of the transitions are not changed, the energy levels involved in the transitions are not changed. How do the anomalous intensities arise? Since they do not arise from anomalies in energy levels, they must arise from anomalies in the populations of the levels, that is, from deviations of the electron spin Zeeman levels from the Boltzmann (thermal or equilibrium) population. We now consider how this can come about during a photochemical reaction.

1.4.1. The Spin Level Population Basis of ESP

The concepts of ESP and deviations from Boltzmann distributions are not familiar to most organic chemists and, therefore, a simple but hopefully clarifying discussion of ESP is warranted. The EPR signal intensity is proportional to the difference in the populations of the energy levels (Δn) involved in the observed transitions between magnetic sublevels. This energy difference is very small (typically the excess of the lower level is less than 1 part in 10000) in conventional EPR where spin systems are in thermal equilibrium (because $\Delta E_{Zeeman} \ll k_B T$ at room temperature). However, we shall see that there are several mechanisms commonly occurring in photochemical reactions which produce ESP in an elementary step or sequence of elementary steps.

A convenient and practical experimental definition of ESP is the deviation of an instantaneous population of spins from the equilibrium (Boltzmann) population at a given temperature. At the resonance frequency, the oscillating field of electromagnetic radiation stimulates both upward and downward transitions between energy levels. The probabilities and experimental intensities of upward and downward transitions depend on the difference in the populations of the energy levels. Thus, the phenomena of ESP can be investigated through measurements of the deviations of the intensities of EPR transitions from those expected for Boltzmann populations, and TREPR spectroscopy (which measures instantaneous populations of spins) can be employed to measure ESP. Since ESP does not affect the energy difference between spin levels, the frequency of the EPR transitions is not influenced by the degree of ESP. Thus, the TREPR technique does not influence the structural information (energy differences between levels) that is obtained in systems for which ESP occurs. Experimentally, the TREPR study of radicals produced by nanosecond laser flash photolysis very shortly after

their formation demonstrates that often the radicals possess significant ESP. The extent of spin polarization may be dependent on the hyperfine level, that is to say that, lines corresponding to different nuclear spin states may be polarized to different extents. These unusual patterns created by different polarization mechanisms carry information on both the history of the "parents" of the observed radical pairs and their "children" radicals. These mechanisms will be discussed together with examples in the sections below.

1.4.2. Schematic Description of the Influence of ESP on EPR Spectra

Scheme 5 shows the concept of ESP schematically for a doublet state in a strong magnetic field. Scheme 5b represents the spin system at equilibrium. The population of the two spin sublevels is nearly equal, and this near equality is indicated by

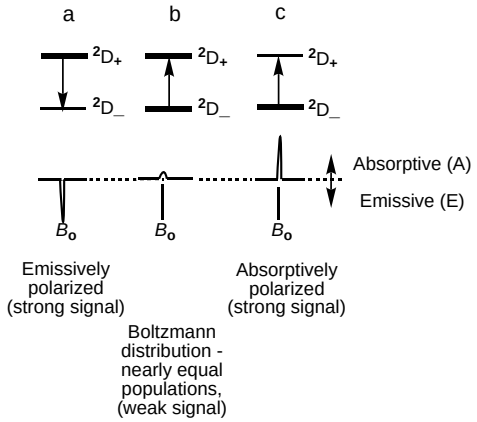

Scheme 5. Schematic representation of Boltzmann (b) and spin-polarized [(a) and (c)] magnetic sublevels and corresponding EPR transitions for a doublet state. The thickness of the lines in the energy diagram refers to the population of the state (a thicker line implies a larger population). The field position of the signal is identical in all cases at B_0; the differences are in the intensities of the signals. See text for a more complete description.

a line of the same thickness for both $^2D_+$ and $^2D_-$ levels. In fact the EPR signal at B_0 observed in a conventional steady-state experiment is the result of the small excess of spins in the $^2D_-$ level. If we use the equilibrium population as a reference state, then any deviations from this population in either direction may be defined as a polarized population.

Now consider the situation of the $^2D_+$ level being overpopulated through some process (Scheme 5a, where the overpopulation is indicated by a thicker line for the $^2D_+$ level). If the EPR measurement is made while $^2D_+$ is overpopulated, instead of a weak absorption at B_0 arising from the overpopulation of $^2D_-$, a net emissive phase signal (termed E) is observed at the same frequency (B_0) as for the system at the Boltzmann distribution (Scheme 5b). If the EPR measurement is made while $^2D_-$ is overpopulated (Scheme 5c), instead of a weak absorption at B_0 arising from the overpopulation of $^2D_-$, an enhanced absorption phase (termed A and implying that the measured intensity is stronger than that expected for the Boltzmann population of the energy levels) is observed at the same frequency, B_0.

1.5. ESP and Chemically Induced Dynamic Electron Polarization

Anomalous EPR signals arising from electron spin polarization (ESP) are lumped under the general term CIDEP (chemically induced dynamic electron polarization) spectra, although, strictly speaking, ESP can be produced by several origins. Indeed, there exist ESP mechanisms which are neither "chemically induced" (that is, by bond breaking or bond forming) nor "dynamic" (diffusion of radicals). There are many examples where nonreactive encounters of triplet excited molecules with doublet free radicals generate ESP.[15] For example, excitation of a chromophore that is covalently linked to a stable free radical, results in a strong ESP that does not rely on diffusive encounters of the triplets and the doublets. Therefore, we prefer using the simple name electron spin polarization (ESP) and the spectra observed can be termed ESP-TREPR spectra. The observation and interpretation of ESP in TREPR spectra observed during photochemical reactions will be discussed to provide important information concerning the entities involved in photochemical reactions and in elucidating the mechanisms of transformations of these entities.

As mentioned above, ESP-TREPR spectra differ only in the intensities of the "lines" but not in the number of lines or in the frequencies of the lines. Thus, the interpretation of the structure of the species responsible for the spectrum is generally unambiguous. The lifetime of ESP is usually limited by the time needed for the spin population to relax to the Boltzmann distribution, which is, typically, of the order of microseconds in nonviscous liquid solutions. Equipment capable of detecting signals on the submicrosecond time scale is, therefore, essential because of this rapid decay time.

ESP in the measurement of TREPR signals has both technical and scientific advantages. At the technical level, the electron spin polarization creation (ESPC) is a wonderful bonus in that ESP creates a powerful signal-to-noise advantage in measurements of $^3T_1$, ^3RP, and ^2FR (compare with Scheme 2). It is this signal-to-noise advantage resulting from ESP which allows the detection of very low concentrations of paramagnetic entities on the submicrosecond timescale in TREPR experiments. In fact, this signal-to-noise enhancement more than compensates for the loss of signal-to-noise arising from the lack of phase sensitive detection (compare with Section 1.6). At this point, a word of caution is required because of the inherent sensitivity and selective observational powers of this technique. The observation of the TR-ESP spectrum derived from a polarized, paramagnetic product cannot rule out the formation of other "EPR-silent" products. It is always best to use multiple techniques in order to fully characterize the reactive intermediates and products, as well as to draw mechanistic conclusions. Furthermore, at the scientific level, the ESPC and electron spin polarization transfer (ESPT) allow definitive identification of the predecessors of paramagnetic entities and the transitions leading to these entities, thereby providing important mechanistic information on both the entities and transitions involved in photochemical reactions.

1.6. Comments on the Experimental Instrumentation of TREPR

It is relatively straightforward to modify a conventional, commercial EPR spectrometer to operate in the time-resolved mode.[1, 5, 11] The requirements are the addition of a boxcar integrator, the availability of a pulsed laser, a trigger diode, and a fast preamplifier for the microwave bridge. Such a modified instrument will have a response time in the range of 100 ns. Recently, Elger et al. have introduced an X-band spectrometer with time resolution of about 10 ns.[16] Radicals possessing ESP polarization are produced in the cavity of the spectrometer by a short (ca. 10 ns) laser pulse, and the EPR transitions are observed with nanosecond time resolution in a fixed external magnetic field B_0. The transient EPR signals are integrated within a set time window using the boxcar integrator, to yield a single point in the spectrum. The integration window typically starts from 0.1 to a few microseconds following the laser flash, and is open for a few hundred nanoseconds. To obtain an entire spectrum, the external magnetic field is varied incrementally and the measurements are repeated a number of times and averaged to obtain an acceptable level of signal-to-noise. It is an important technical point that TREPR spectra are represented in a direct mode rather than the first derivative form that is typical of steady-state EPR. The spectra thus have an appearance which is closer to that of NMR spectra in that each transition appears as a conventional signal rather than the derivative of the signal.

1.7. Summary

The immersion of the paramagnetic species in the photochemical paradigm of Scheme 2 into a magnetic field causes a splitting of $^3T_1$ and ^3RP into three magnetic sublevels, termed $^3T_+$, $^3T_0$, and $^3T_-$, and causes a splitting of ^2FR into two doublet states, $^2D_+$ and $^2D_-$. The photochemical paradigm of Scheme 2 is now "enriched" in the number of entities and transitions that must be considered along a photochemical pathway which is followed in a strong magnetic field. A set of spin selection rules is also added to the paradigm. It is now natural to ask whether the spin selection rules are followed in photochemical reactions. We shall show how ESP, together with TREPR, provides an outstanding tool for answering this question. Having provided a basis for discussing EPR spectra and the background for the concept of ESP, next we will discuss ESP, and how it may be created, sorted, and transferred.

2. Electron Spin Polarization Creation and Transfer

2.1. An Exemplar Paradigm of Organic Photochemistry: The Photochemical α-Cleavage of Carbonyl Compounds

The photochemistry of carbonyl compounds and especially of ketones provides photochemists with a particularly mature and useful set of working and exemplar paradigms.[5, 17, 18] We now seek to describe experimental systems involving ketones and carbonyl compounds for which the TREPR technique will provide penetrating tests of the validity of these working and exemplar paradigms. The working paradigm for ketones teaches that the primary photochemical processes of ketones ($^*R(^3T_1) \rightarrow I(^3RP)$, Scheme 2) usually occur from triplet n,π* states [$^3T_1$ (n,π*)] of ketones. The paradigm[17] further teaches that there are only about four commonly observed primary photochemical processes of T_1(n,π*) states: 1) hydrogen abstraction; 2) electron abstraction; 3) addition to double bonds, and 4) α-cleavage. Of these primary photochemical processes, in this account we shall use α-cleavage (a well-studied unimolecular reaction which produces geminate triplet radical pairs in high yield in both molecular and supramolecular systems) and the subsequent secondary processes involving the dynamic radical pair (Scheme 2) as a working paradigm for the photochemistry of ketones. The α-cleavage reaction, in turn, will serve as an exemplar for the use of TREPR and electron spin polarization to investigate photochemical reactions in molecular and supramolecular systems.

An exemplar paradigm for α-cleavage is readily derived from the working paradigm for the photochemistry (Scheme 2). In the exemplar paradigm (Scheme 6) we replace $^1S_1$, $^3T_1$, ^3RP, ^2FR, and ^1RP with the appropriate structures of a ketone AC(O)B, which undergoes a primary photochemical α-cleavage of the C(O)-B bond. For simplicity's sake at this point, we consider that the only products are those that result from combination reactions of radical pairs. We will consider scavenging reactions of free radicals in Section 2.4.

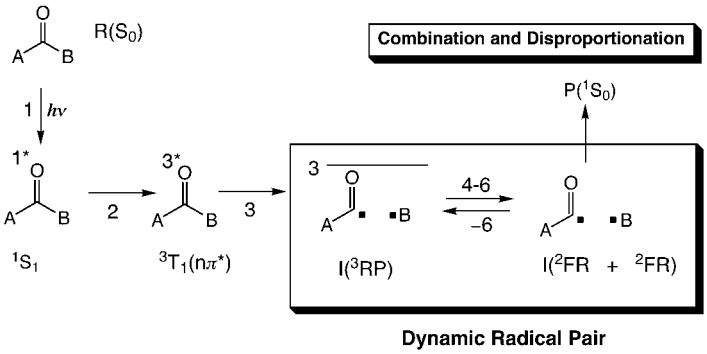

Scheme 6. An exemplar paradigm for the α-cleavage of carbonyl compounds. Excitation of a ketone to an n,π* triplet excited state leads to α-cleavage and the formation of a dynamic radical pair. See text for discussion.

Let us consider the features of Scheme 6 that are relevant to TREPR, namely the paramagnetic species and the transitions involving paramagnetic species:

1) Step 2 is an efficient and rapid intersystem crossing from $^1S_1$ to $^3T_1$(n,π*) of the ketone AC(O)B. This step converts $^1S_1$ (a diamagnetic, EPR "silent" species) into $^3T_1$ (a paramagnetic, EPR "active" species). TREPR spectroscopy allows the direct spectroscopic investigation of the structure of $^3T_1$(n,π*) and an indirect investigation of the mechanism of spin creation ($^1S_1$ has spin zero; $^3T_1$ has spin one) through examination of the spin sublevel selectively

of the ISC process. The latter produces an electron spin polarized $^3T_1$ state of the ketone. This polarization can be employed to track the subsequent processes involving paramagnetic species indicated in Scheme 6.

2) Step 3 is a primary photochemical α-cleavage of $^3T_1$ of the ketone to produce a geminate, triplet radical pair $^3(ACO^{\bullet}\ {}^{\bullet}B)$, which is usually not directly detectable in nonviscous solvents, because the timescale of separation (ca. 100 ps) of the geminate radical pair into free radicals ($^2ACO^{\bullet}+{}^2B^{\bullet}$, step 4) is much faster than the response time of the TREPR technique (ca. 100 ns).[*] However, in supramolecular systems, such as micelles, $^3(ACO^{\bullet}\ {}^{\bullet}B)$ may possess a lifetime that is accessible to TREPR spectroscopy, as will be discussed in Section 3.4.2.
3) Step 4 involves the separation of the geminate pair to produce spin uncorrelated free radicals $^2ACO^{\bullet}+{}^2B^{\bullet}$ that are readily investigated directly by TREPR spectroscopy provided that the radicals carry polarization generated from step 2 or 3 (or some other mechanisms, see Section 2.5).
4) In subsequent steps (step 5 and 6 in Scheme 2 and Scheme 6), the free radicals formed in step 4 eventually reencounter in a random fashion (compare with the more general situation for the dynamic radical pair of Scheme 2) and form random radical pairs—75% of the time to form unreactive triplets $^3(ACO^{\bullet}\ {}^{\bullet}B)$ and 25% of the time to form reactive singlets $^1(ACO^{\bullet}\ {}^{\bullet}B)$). The singlet radical pairs react to yield products by radical–radical recombination reactions and the triplet radical pairs separate to become free radicals again. The latter continue to cycle through reencounters to produce $^3(ACO^{\bullet}\ {}^{\bullet}B)$ and $^1(ACO^{\bullet}\ {}^{\bullet}B)$. We will see that the dynamic radical pair may be investigated by TREPR spectroscopy in both nonviscous solvents and in supramolecular systems such as micelles.

In addition to the information discussed above, TREPR spectroscopy will be shown to be a powerful method for investigating the reactions of the free radicals produced in step 4 and, in micellar systems, to study the electron exchange (J) and the supramolecular interactions between the radicals of the geminate pair.

In the following sections we will first show how the TREPR technique can be employed to investigate the transitions $^1S_1 \rightarrow {}^3T_1$ and $^3T_1 \rightarrow {}^2FR$ as well as to demonstrate the validity of the spin-selection rules for step 2–4. After that, we will show how the ESP produced in the $S_1 \rightarrow T_1$ step might be transferred through collisions and reactions and how these processes may be monitored by TREPR spectroscopy. We will also show how to employ supramolecular concepts to slow down the $^3RP \rightarrow {}^2FR$ step so that the lifetime of the radical pair is long enough to observe ^3RP directly by the TREPR technique. Finally, we will present some selected examples of the use of TREPR spectroscopy to elucidate some important aspects of supramolecular interactions between radicals.

[*] Throughout the text a "+" between two radicals will indicate free radicals. Geminate radicals will be indicated by inclusion in parentheses without the "+" between the structures.

2.2. Application of the TREPR Technique to an Exemplar Paradigm of Photochemical α-Cleavage of Carbonyl Compounds

The paradigm of spin mechanics specifies as a fundamental principle that for all elementary processes the total spin must be conserved, and for elementary processes in a magnetic field the projection of spin on the axis of magnetization must be conserved. This principle is responsible for the selectivity, generation, transfer, and sorting of ESP. We now apply this principle to each of the steps in Scheme 6 and then apply the TREPR technique to experimentally test the validity of the principle through the observation of ESP.

2.2.1. The $^1S_1 \rightarrow {}^3T_1$ Intersystem Crossing

The $^1S_1 \rightarrow {}^3T_1$ transition involves the creation of spin angular momentum (the singlet has no spin; the triplet has a spin of one). Thus, to conserve overall angular momentum there must be a loss of some type of angular momentum in the total molecular system. For aromatic carbonyl compounds it is *orbital* angular momentum that is lost as *spin* angular momentum is created. This exchange of orbital and spin angular momentum is termed "spin–orbit coupling" (SOC) and it is the mechanism which drives the $^1S_1 \rightarrow {}^3T_1$ transition.[17] Because an orbital transition has a specific spatial relationship to the molecular framework, it is plausible to assume that the spin momentum that is created to produce $^3T_1$ will also have a specific orientation to the molecular framework. This orientation can be described in terms of the spin being oriented along one of three Cartesian axes which refer to the molecular frame. When dealing with n,π* transitions of ketones, to a good approximation, the local symmetry about the C=O bond is not very sensitive to substituents so that an axis along the C=O bond can serve as a reference (z-axis). Furthermore, the SOC for carbonyl compounds can be viewed as a one-center orbital interaction localized at the oxygen atom. This implies that the SOC is largely determined by the local symmetry of the C=O group. It can be shown[5] from such considerations that the SOC along a z-axis which corresponds to the C=O bond is strongest for a $\pi \rightarrow$n interaction. This z-axis is also termed the spin quantization axis.

The most favorable orbital situation for SOC for a ketone is shown schematically in Scheme 7. The greatest degree of orbital angular momentum is generated along the C=O bond near the oxygen atom when n $\rightarrow\pi$ orbital motion occurs, for example, during molecular vibrations. Coupling of the orbital motion of a π electron with the motion of the spin of the electron in the n orbital "flips" the spin of the n electron and creates a triplet state and spin along the z-axis. In terms of state mixing, such an interaction corresponds to mixing of a $^1S_1(n,\pi^*)$ state with a $^3T_1(\pi,\pi^*)$ state. For aromatic ketones there is generally an energetically accessible $^3T_1(\pi,\pi^*)$ state which lies close to the chemically reactive n,π* state.

The basic idea in the spin–orbit coupling mechanism is that the orbital angular momentum must change by one unit at the same time that the spin angular momentum changes by one unit so that the total change in angular momentum is zero. This idea is depicted schematically in Scheme 7, of which the

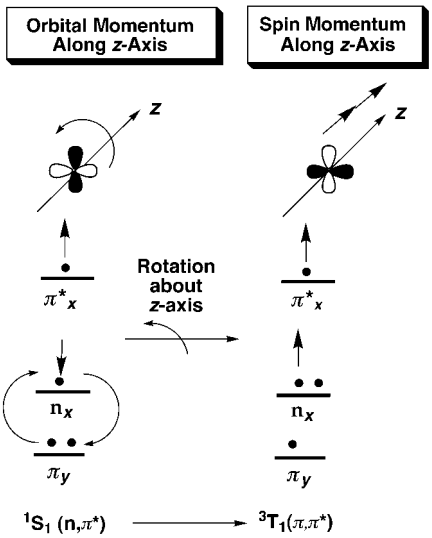

Scheme 7. SOC-induced $S_1 \rightarrow T_1$ ISC of a ketone possessing a lowest energy $^1S_1(n,\pi^*)$ state. See text for further discussion.

left hand side shows the $^1S_1(n,\pi^*)$ state. Orbital motion corresponding to the $n \rightarrow \pi_y$ rotation generates orbital angular momentum about the *z*-axis. This orbital motion couples to the spin motion of the electron in the n orbital, so that there can be a decrease in the orbital angular momentum from 0 to -1 (or 1 to 0) and an increase in the spin momentum from 0 to 1. This effect corresponds to a singlet to triplet transition and an intersystem crossing from $^1S_1$ to $^3T_1$. Total angular momentum is conserved and the spin selection rules are obeyed. The mixing is strongest when the full π_y electron is transferred to the n orbital (El-Sayed's Rule).[17] When this happens a $T_1(\pi,\pi^*)$ state is produced.

2.2.2. Sublevel Selectivity of ISC—ESP Creation

Intersystem crossing (ISC) from an excited singlet to a triplet state always takes place in accord with "spin selection rules" that operate in the molecule. If ISC occurs in the magnetic field of an EPR spectrometer we can imagine the applied field being so strong that it couples with the spin vector in the molecule and causes the spin vector to line up with the laboratory magnetic frame. In this case, the resulting triplet will be formed predominately in one of the triplet sublevels, $^3T_+$, $^3T_0$, or $^3T_-$, (see Scheme 4) with the total electron spin oriented along one of the principle molecular axes of the ketone.

According to this model the orbital motion which is directed along the *z*-axis (C=O direction) is transformed selectively into spin motion along the *z*-axis, that is, as orbital angular momentum is selectively destroyed along the *z*-axis, spin angular momentum is created selectively along the *z*-axis (shown in Scheme 7 as two arrows pointing along the *z*-axis). From detailed calculations for aryl alkyl ketones, this simple model predicts that the highest energy magnetic sublevel $^3T_+$ (using the high field notation) will be selectively populated by ISC from $^1S_1$ to $^3T_1$, thus generating ESP in this level. Depending on the detailed structure and local symmetry of the carbonyl group, either $^3T_+$ or $^3T_-$ can be selectively populated by ISC. This rather remarkable prediction is readily tested by experimental examination of the TREPR of $^3T_1$ states.

2.3. EPR Spectroscopy of T_1 States—Some General Considerations

From the discussion of selective spin sublevel population by ISC it may be concluded that if an EPR measurement could be made immediately after the intersystem crossing step occurred in a carbonyl compound and before spin lattice relaxation brings the spin-polarized triplet to the Boltzmann distribution, the observation would be an emissive signal from $^3T_+$ to $^3T_0$ or an enhanced absorption from $^3T_-$ to $^3T_0$. Scheme 8 shows schematically the sublevel-selective ISC from

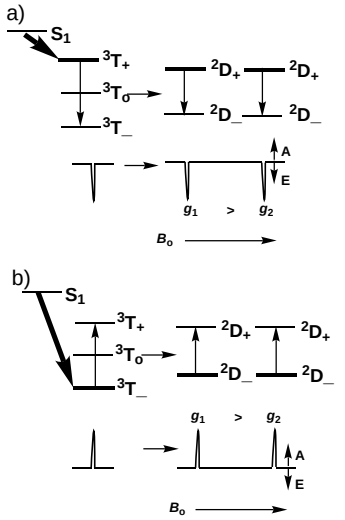

Scheme 8. Schematic drawing of the magnetic level diagram for producing ESP through the $^1S_1 \rightarrow {}^3T_1 \rightarrow {}^2D + {}^2D$ process (triplet mechanism, TM). The ISC selectively occurs to the $^3T_+$ level (a) or to the T_- level (b), which leads to emissive (E) and absorptive (A) polarization, respectively, for the $\Delta m = 2$ transition (at 77 K) and emissive and absorptive polarization, respectively, for the radicals produced by α-cleavage (at room temperature). See text for discussion.

$^1S_1$ to $^3T_1$ for a case in which the $^3T_+$ sublevel (Scheme 8a) or the $^3T_-$ sublevel (Scheme 8b) is populated selectively. In practice, the experimental TREPR spectrum of a molecular triplet is very complex for several reasons. The first complication is the existence of strong dipole–dipole interactions between electron spins, which are coupled to the molecular frame and are, therefore, very strong in a molecular triplet state. Furthermore, in an EPR spectrometer these interactions are modulated by the tumbling of the triplet species in a magnetic field. This modulation, in turn, causes a fast spin-lattice relaxation of the triplet sublevels. At room temperature the rate of spin-lattice relaxation of the triplet sublevel is of the order of 1 ns for nonviscous solutions.[19]

Since the time resolution of TREPR operating in the continuous wave (CW) mode is of the order of 100 ns, this technique cannot be used to probe the population of the selective triplet sublevel directly in fluid solutions. In addition,

fast relaxation causes extensive line broadening in all magnetic resonance measurements. This line broadening (which causes poor signal-to-noise in the measurements), coupled with a short lifetime of the triplet sublevels makes the direct measurement of the $^3T_1$ state in solution by TREPR very difficult, even for spin-polarized triplet species. Only in a few cases has the TREPR of molecular triplets been observed in nonviscous liquids.[20, 21]

In order to observe the predicted selective population of triplet sublevels by EPR, the measurement must be made before spin-lattice relaxation occurs and the sublevels attain the Boltzmann population. Immobilization of a molecular triplet in a transparent glass at 77 K (or lower) removes the problem of a short spin relaxation. However, there is a price to be paid for extending the triplet lifetime. In a rigid matrix, a triplet state consists of molecules randomly distributed in a large number of different orientations which are interrogated during a measurement. This situation leads to a very broad signal spanning over 4000 G for organic molecules, whereas the typical width for an EPR spectrum of a carbon-centered free radical is 100 G. In spite of these complications, when $^3T_+$ or $^3T_-$ are produced spin polarized as a result of sublevel selective ISC, the TREPR spectrum can readily be observed in rigid matrices that eliminate rotation and slow down spin-lattice relaxation. Furthermore, the magnetic parameters of the triplet state and the sublevel population ratios may be conveniently determined by comparing the observed spectrum with computer simulated spectra, and the matter of whether $^3T_+$ or $^3T_-$ is selectively populated can be resolved.

In actual experimental cases of ketones it has been found that the EPR transitions between $^3T_-$ and $^3T_+$ (so-called $\Delta m = 2$ transitions, see Scheme 8) are readily observed because of mixing of $^3T_0$ with the adjacent sublevels. This is important because the position of the $\Delta m = 2$ transition turns out to be relatively insensitive to the orientation of the triplet in the magnetic field, so a relatively sharp transition is observed.

2.3.1. Experimental Examples of TREPR of T_1—ESP of T_1 by ISC

Figure 1 shows examples of the entire TREPR spectra of benzoin (**1a**)[22] and diphenyl(2,4,6-trimethylbenzoyl)phosphine oxide (**2**) at 77 K[23] and the associated simulated

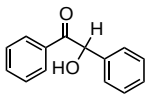

1a

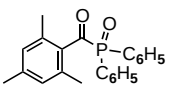

2

spectra. At this temperature spin-lattice relaxation of the sublevels is of the order of a microsecond or longer. A $^3T_1$ state is produced with a nanosecond laser and then a TREPR spectrum is accumulated by boxcar integration in a microsecond or less.

The entire TREPR spectra of Figure 1 are spin polarized. The $\Delta m = 2$ transitions appear at about 1300 gauss in both spectra. In the case of **1a** the $\Delta m = 2$ transition is emissive, corresponding to a polarized $^3T_+ \rightarrow {}^3T_-$ EPR transition, which

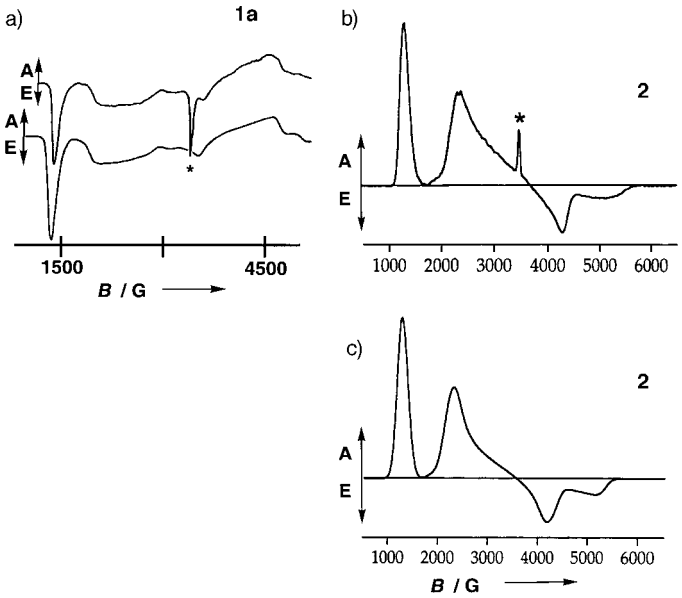

Figure 1. TREPR spectra of benzoin (**1a**) at 77 K (a; top: experimental, bottom: simulated) and diphenyl(2,4,6-trimethylbenzoyl)phosphane oxide (**2**; b: experimental, c: simulated). The sharp line indicated by the asterisk (*) arises from to a carbon-centered radical produced by photolysis.

is consistent with the selective population of the $^3T_+$ state by ISC from $^1S_1$ (Scheme 8a). On the other hand, in the case of **2**, the $\Delta m = 2$ transition is in enhanced absorption, corresponding to a polarized $^3T_- \rightarrow {}^3T_+$ transition Scheme 8b. Thus, we have two carbonyl compounds capable of undergoing α-cleavage to produce ESP in different phases: For **1a**, ISC selectively populates $^3T_+$ (emissive phase), and for ketone **2** ISC selectively populates $^3T_-$ (enhanced absorptive phase). The excellent agreement of simulated and experimental spectra (Figure 1a, lower spectrum, Figure 1c) confirm the assignments of the selective overpopulations.

Although the ESP generated in the $^1S_1 \rightarrow {}^3T_1$ ISC step for **1a** or **2** is not directly detectable by the TREPR technique at room temperature in fluid solution, it is reasonable to ask whether the selective population of triplet sublevels occurs under these conditions. In the next section we shall see how the TREPR technique answers this question indirectly but unambiguously, and how the ESP generated in the ISC step may be exploited by this technique to further examine the paradigm of Scheme 6.

2.3.2. Correlation of the TREPR of Molecular Triplets with Primary Photochemical Processes—The Triplet Mechanism of ESP

We have seen how a photophysical process, the intersystem crossing from a singlet state to a triplet state, can be investigated by TREPR spectroscopy at 77 K. Thus, $^3T_1$(**1a**) and $^3T_1$(**2**) are "born" spin polarized in $^3T_+$ and $^3T_-$, respectively, and that ESP is created by the ISC transition. We now follow the magnetic level correlation diagram of Scheme 4 and note the consequences of the spin-selection rules for elementary primary photochemical α-cleavage. If the polarization found by TREPR (Figure 1) at 77 K is carried over at room temperature, and if α-cleavage can occur within

the spin-lattice relaxation time of the triplet state (ca. 1 ns),[19] then **1a** and related ketones should produce electron-spin polarized $^2ACO^{\#}$ and $^2B^{\#}$ radicals that can be observed in emission, and **2** (and related compounds) should produce electron spin polarized radicals that can be observed in absorption because angular momentum must be conserved (the superscript # signifies a polarized electronic spin). The general schemes for these two possibilities is shown in Scheme 8a and b, respectively, while the experimental results obtained in fluid solution at room temperature are shown in Figures 2 and 3.[24]

In the case of **1b**, an emissively (E) polarized benzoyl radical (a broad triplet with $g = 2.001$, indicated by the arrow in Figure 2a) and an emissively polarized ketyl radical (seven lines, with $g = 2.003$) are observed in the TREPR spectrum. All of the lines are in net emission (E), consistent with the selective ISC of $^1S_1$ to $^3T_1$ to form $^3T_+$ followed by rapid α-cleavage of $^3T_+$ to form $^2D_+$. The triplet mechanism (TM) is the term given to the process in which spin polarization is produced through a primary photochemical reaction of a triplet excited state whose sublevels are polarized by ISC.

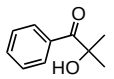

1b

In the case of **2**, an absorptively (A) polarized benzoyl radical (a broad triplet with $g = 2.001$, indicated by the arrow in Figure 3a) and an absorptively polarized phosphorous centered radical (a doublet, with $g = 2.003$) are observed in the TREPR spectrum. The polarization produced by the photolysis of **2** contrasts with the polarization produced in the photolysis of **1b**, that is, all of the lines in the TREPR spectrum of **2** are in net absorption (A), which is consistent with ISC of $^1S_1$ to $^3T_1$ to form $^3T_-$ selectively, followed by rapid α-cleavage of $^3T_-$ to form D_-.

A careful inspection of Figures 2a and 3a reveals that the polarization is not exactly symmetrical at low field (left) and high field (right). This is a common situation that arises from other polarization mechanisms occurring in addition to the TM, which should generate a completely symmetrical polarization pattern. One of these other mechanisms that can produce spin polarization, the radical pair mechanism (RPM), will be discussed in Section 2.5.

Thus, we have two exemplars of α-cleavage of carbonyl compounds that demonstrate the ability of the TREPR technique to track ESP produced by sublevel-selective ISC through to the free radicals produced by the primary photochemical process. The combination of ESP and TREPR provides a means of unambiguous direct observation and identification of the ^2FR species produced by a primary photochemical process through measurement of hfc and g-values. In addition, ESP-TREPR spectra provide a means of indirectly determining the spin characteristics of the *R species that underwent cleavage through the observation of the phase of the ESP. The observation of TM ESP confirms the paradigm expectation that the primary photochemical process occurs from a triplet state (step 3 in Scheme 2 and 6).

We next consider how TREPR and ESP can be used to track secondary reactions involving radical scavenging and to elucidate the intermolecular interactions of the partners of a dynamic radical pair.

2.4. TREPR Investigations of ESP Transfer from Primary Spin Polarized Reactive Radicals Produced by α-Cleavage to Secondary Scavenging Reactions—Reactive ESP Transfer

We have seen above in Section 2.3 that the polarization created in spin-selective ISC from $^1S_1$ to $^3T_1$ is carried over to produce polarized $^2ACO^{\#}$ and $^2B^{\#}$ radicals formed in the α-cleavage of AC(O)B*. In these cases the polarization generated in a specific sublevel of a parent $^3T_1$ serves firstly to label the daughter radicals produced by a photochemical event, secondly to enhance the signal-to-noise of detection of the daughter radicals, and thirdly to provide definitive evidence on the origin of the precursor of the daughter radicals. In many photochemical reactions the radicals produced in the primary photochemical process are scavenged by reactions with molecules (secondary processes) to produce secondary radicals [Eqs. (2) and (3)].

$$^2ACO^{\#} + \text{scavenger} \longrightarrow \text{ACO-scavenger}^{\#}\ (^2FR_a^{\#}) \quad (2)$$

$$^2B^{\#} + \text{scavenger} \longrightarrow \text{B-scavenger}^{\#}\ (^2FR_b^{\#}) \quad (3)$$

It is natural to inquire whether the expected spin-selective scavenging reactions that produce spin-polarized secondary radicals can be detected by TREPR spectroscopy. The requirement for observing polarized radicals from scavenging reactions is that the rate of the scavenging reaction is faster than the spin-lattice relaxation of the parent polarized free radical. Since the spin-lattice relaxation of carbon-centered free radicals[1] is of the order of $1-10\ \mu s$, the scavenging reaction must be of this order of magnitude or faster. Thus, in favorable cases, ESP may serve as a "tracer" or a very subtle and noninvasive "label" of radical reactions. The process of transfer of polarization from a $^2FR^{\#}$ radical to a new radical by reaction is termed reactive ESP transfer (ESPT). Since the spin-selection rule for ESP is expected to operate in the elementary step of a reaction of a radical with a molecule, the phase of the polarization of the primary ^2FR radical is expected to be transferred to the secondary radical produced by scavenging [Eqs. (2) and (3)]. Of course reactions of two ^2FR radicals produce diamagnetic molecules (P in Scheme 6) which are not detected by EPR.

2.4.1. Examples of a TREPR Investigation of Reactive ESPT—Secondary Reactions of Free Radicals Produced in Primary Photochemical Processes

Carbon-centered radicals produced by photochemical α-cleavage of carbonyl compounds such as **1b** and **2** are scavenged by ethylenes in the photoinitiation step in free radical polymerization. The photolysis of **1b** and **2** produces polarized $^2ACO^{\#}$ and $^2B^{\#}$ radicals, and if the free radical can add to the olefinic monomer within the spin relaxation time of the polarized radical then the addition of these radicals to ethylenes is expected to generate spin-polarized adducts. For example, Equations (4) and (5) show the addition of the fragments from α-cleavage of a polarized ketone to methyl methacrylate (MMA), an important monomer in photoin-

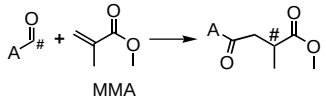

(4)

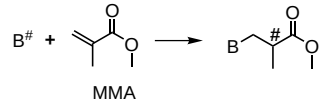

(5)

duced free radical polymerization. The issue to be considered by TREPR spectroscopy is whether the polarization of the $^2ACO^{\#}$ and $^2B^{\#}$ species that is produced by TM is carried over to the new radicals formed by the scavenging of the radicals. The expectation from spin-selection rules is that since the parent radicals produced in the photolysis of **1b** (Figure 2a) are emissively polarized, the scavenged radicals produced from **1b** will also be emissively polarized. Similarly, since the parent radicals produced from the photolysis of **2** are produced in enhanced absorption, the scavenged radicals produced from **2** will also be absorptively polarized. These expectations are confirmed in Figures 2 and 3.

Figure 2[24] shows the TREPR spectrum produced by photolysis of **1b** in acetonitrile in the absence (Figure 2a) and presence (Figure 2b, c) of MMA. A simulated spectrum (Figure 2d) for the adducts of $^2ACO^{\#}$ and $^2B^{\#}$ to MMA (of which both spectra are essentially identical) is also shown.

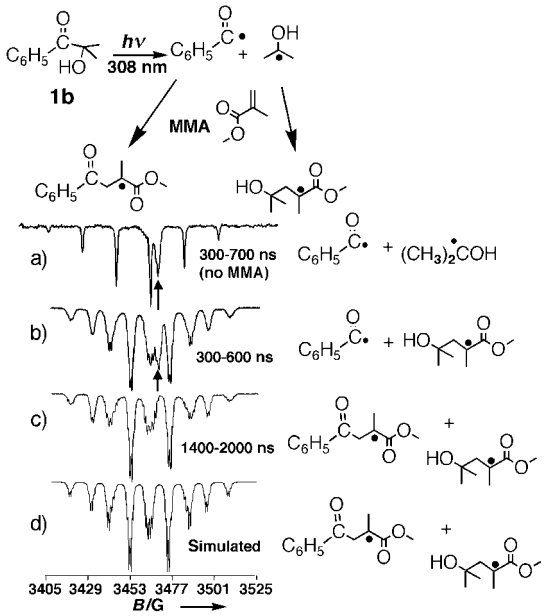

Figure 2. ESP-TREPR spectrum resulting from the photolysis of **1b** in acetonitrile (a), or in MMA 300–600 ns (b), 1.4–2 μs after the laser flash (c) as well as the simulated spectrum of the radical adduct with MMA (d). The arrow points to the signal derived from the $^2ACO^{\#}$ radical.

From the simulation it is clear that the radicals present after 2 μs arise from the addition of ACO and B to MMA. In addition, the observed E polarization of the radical produced by scavenging is the same as that of the primary parent precursor. The observation of transfer of emissive ESP from the primary radicals to the secondary radicals confirms that the spin angular momentum is conserved in the addition step.

In addition to confirming the spin-sublevel selectivity of the addition of radicals to ethylenes, there is further mechanistic information that can be extracted from the experimental spectra. For example, from Figure 2b it is noted that the addition of the $^2B^{\#}$ radical is complete within a few hundred nanoseconds. This observation implies that the rate constant for addition of $^2B^{\#}$ to MMA is of the order of $10^6-10^7\,M^{-1}s^{-1}$, a value consistent with the value of $10^7\,M^{-1}s^{-1}$ reported in the literature.[25] It is also noted that the addition of the $^2ACO^{\#}$ radical to MMA is about an order of magnitude slower, since some of the polarized $^2ACO^{\#}$ radical has still yet to react after about 500 ns (arrow in Figure 2b). However, the signal corresponding to $^2ACO^{\#}$ is gone after approximately 1500 ns.

The rate constant for propagation of MMA is approximately $10^2\,M^{-1}s^{-1}$, which is much slower than for the addition of either radical to MMA monomer, so that even in MMA solvent (ca. 10 M) it is expected that the second propagation step will be too slow to detect by TREPR spectroscopy at the integration times employed. Thus, the observed radical produced by addition of polarized radicals is expected to be only the first adduct produced by scavenging of the primary radicals, but this cannot be demonstrated with this experiment since the tertiary radical and other oligomeric radicals produced by polymerization would be expected to have a spectrum essentially identical to the secondary radical.

We now consider the spectrum produced by MMA scavenging (Figure 3a–c) of the polarized radicals produced by photolysis of **2**. A simulation of the spectrum expected if the polarized radicals $^2(C_6H_5)_2P{=}O^{\#}$ add to MMA is shown in Figure 3d. First, we note directly from the spectra that $^2ArCO^{\#}$ adds more slowly to MMA than $^2(C_6H_5)_2P{=}O^{\#}$, since the signals at high and low field arising from $^2(C_6H_5)_2P{=}O^{\#}$ are completely gone after about 300–700 ns, whereas the signal for $^2ArCO^{\#}$ persists (Figure 3b). This observation is consistent with the higher reactivity of $^2(C_6H_5)_2P{=}O^{\#}$ than $^2ArCO^{\#}$ toward MMA. We note also that a comparison of Figures 2b and 3b implies that if acyl radicals are produced from two independent sources of different polarization, their chemical reactivity is unaffected.

Since the phosphorous hfc can be observed in the first adduct to MMA, it was of interest to determine if, at the longest times of observation, the TREPR technique can be used to observe transfer of polarization to the scavenging of the secondary radical by MMA. In fact, this was not observed, presumably the rate of propagation of polymerization of MMA is too slow that the second addition occurs after loss of polarization of the secondary radical. However, polarization transfer has been tracked through two addition steps in the case of the addition of $^2(C_6H_5)_2P{=}O$ to isoprene.[26, 27] The first radical formed upon addition to isoprene shows a clear phosphorous hfc. At later times the phosphorous hfc disappears as the initially formed radical adds to a second monomer. In this case the addition of the first-formed radical to a second monomer is sufficiently fast to occur before the spin polarization has disappeared.

Thus, through the exemplar paradigm of the photochemical α-cleavage of carbonyl compounds with specific examples of **1b** and **2**, we have shown how the TREPR technique is an excellent tool for experimentally observing 1) the creation of

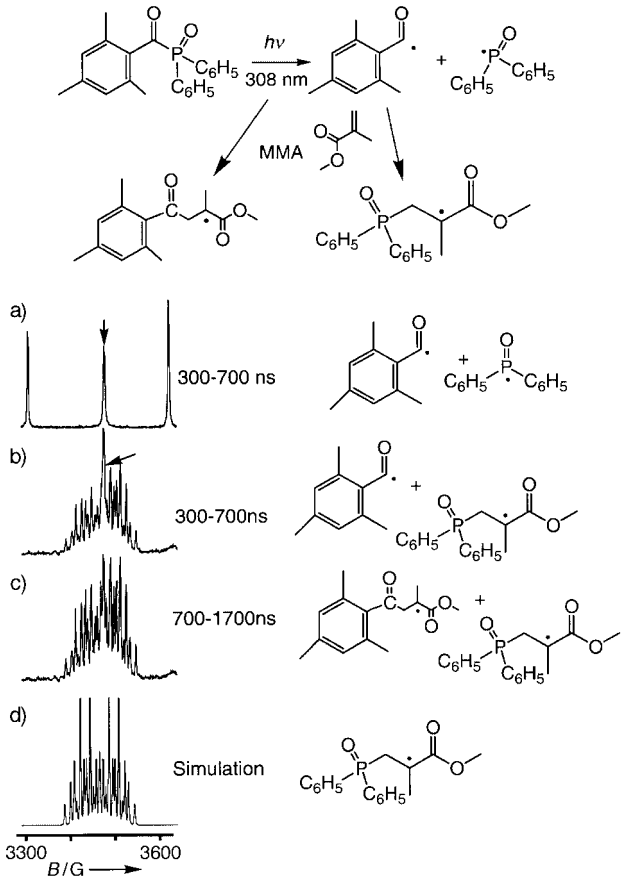

Figure 3. TREPR spectrum resulting from the photolysis of **2** in acetonitrile in the absence (a) and presence (b, c) of MMA. a), b) 300–700 ns after laser excitation; c) 700–1700 ns after laser excitation; d) simulation of the spectrum expected from the addition of $(C_6H_5)_2P{=}O$ to MMA. The arrow points to the signal derived from the $^2ACO^{\#}$ radical.

spin polarization ($^1S_1 \rightarrow {}^3T_1{}^{\#}$), 2) reactive ESPT through a primary photochemical process ($^3T_1 \rightarrow {}^2D^{\#} + {}^2D^{\#}$), and 3) reactive ESPT though secondary scavenging reactions ($^2D_1{}^{\#}$+scavenger$\rightarrow {}^2D_2{}^{\#}$). Next we will show how the TREPR technique can provide information on nonreactive supramolecular intermolecular interactions and collisions between paramagnetic species.

2.4.2. Examples of Nonreactive ESP Transfer Through Intermolecular Interactions of Paramagnetic Species

The working paradigm for organic photochemistry (Scheme 2, box) teaches that, in addition to the combination reactions of free radicals, the dynamic free radical pair involves nonreactive collisions followed by repeated reencounters between free radicals. This is a rather striking feature of the paradigm, since radical–radical reactions between carbon-centered radicals are usually diffusion controlled. Here again the spin-selection rules come into play. Since the primary geminate radical pair (^{3}RP) produced by α-cleavage is a triplet it cannot undergo radical–radical combination reactions, because these reactions produce molecules in a singlet state in an elementary step. However, upon separation of ^{3}RP, two free radicals (^{2}FR) are produced which undergo spin relaxation and then reencounter. The reencountering pairs produce triplet and singlet pairs based purely on spin statistics in a 3:1 ratio. The latter are reactive toward combination reactions and the former are unreactive, and following the collision, the ^{3}RP separate to form free radicals again. The TREPR technique provides a means of investigating the nonreactive collisions of reactants through nonreactive ESP transfer (ESPT).

The basic concept behind nonreactive ESPT experiments is that upon a collision between an unpolarized radical($^2FR^{\bullet}$) and a polarized radical ($^2FR^{\#}$), two possible results may occur as a result of supramolecular interactions: 1) a reactive radical–radical collision (for ^{1}RP pairs) to produce a diamagnetic combination product P($^1S_0$), which is EPR "silent" or 2) a nonreactive radical–radical collision (if the pair is ^{3}RP) followed by separation into free radicals.[28]. During the nonreactive collision, the electron exchange interaction J between the radicals is significant and spin polarization can be transferred from the initially polarized radical to the nonpolarized partner in the pair. Upon separation, the originally unpolarized partner will emerge polarized [Eq. (6)] and the process of nonreactive ESPT can be detected in the ESP-TREPR spectra.

$$^2FR_a{}^{\#} + {}^2FR_b{}^{\bullet} \longrightarrow {}^2FR_a{}^{\bullet} + {}^2FR_b{}^{\#} \qquad (6)$$

These ideas lead to the conclusion that polarized $^2ACO^{\#}$ and $^2B^{\#}$ radicals produced by photolysis of AC(O)B can consequently produce polarization by a nonreactive, electron-exchange mechanism through encounters with any nonpolarized radicals. For example, it is expected from spin-conservation rules that encounters of a nonpolarized free radical with $^2ACO^{\#}$ and $^2B^{\#}$ produced from **1b** will produce an emissive radical (as expected from the results with **1a**) as the result of nonreactive ESPT and that $^2ACO^{\#}$ and $^2B^{\#}$ produced from **2** will produce an absorptively polarized radical as the result of nonreactive ESPT.

Experimental examples of nonreactive ESPT are given in Figure 4. The tack employed is to add TEMPO, a stable,

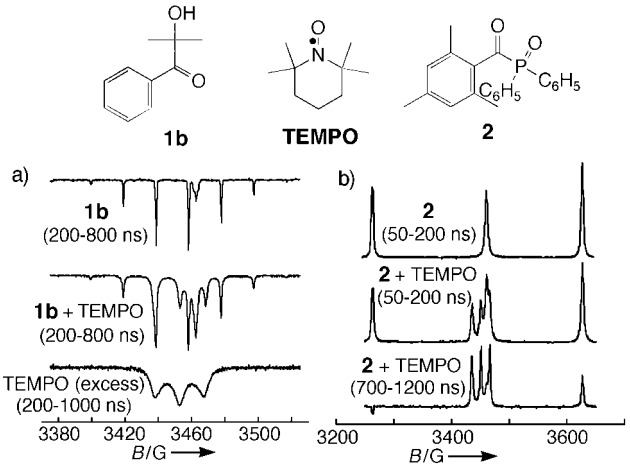

Figure 4. ESP-TREPR spectra demonstrating the nonreactive ESPT. a) An example of the photolysis of **1b** in ethyl acetate. b) An example of the photolysis of **2** in ethyl acetate. A comparison of the spectra in (a) shows it has similar features as the CW-EPR spectrum of TEMPO. The broadening of the signal stems from spin–spin interactions arising from the high concentrations employed.

unpolarized, free radical nitroxide to the sample at a concentration that is too low to be detected by TREPR spectroscopy. If the polarized radicals $^2ACO^{\#}$ and $^2B^{\#}$ that are produced by photolysis of **1b** or **2** encounter TEMPO, collisions will either produce a singlet radical pair (^1RP) that will lead to a diamagnetic product P($^1S_0$), or produce a triplet radical pair (^3RP), which will separate to regenerate free radicals. Since the electron-exchange interaction is significant in ^3RP, some of the polarization of $^2ACO^{\#}$ and $^2B^{\#}$, will be transferred to TEMPO upon separation of the radicals (Scheme 9). Photolysis of **1b** and **2** in the presence of nitroxides leads to the ESP-TREPR spectra shown in Figure 4a and 4b, respectively. It is clear that the expectation of selectivity of polarization transfer is confirmed by the TREPR measurements: Photolysis of **1b** in the presence of TEMPO results in a net emissive spectrum of TEMPO and the photolysis of **2** in the presence of TEMPO leads to a net enhanced absorption spectrum.

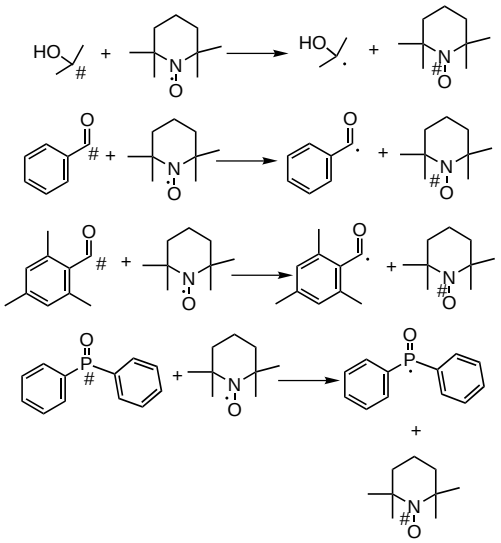

Scheme 9. Nonreactive ESPT between the primary polarized radicals $^2ACO^{\#}/^2B^{\#}$ and TEMPO in the photolysis of 1b (first and second reaction) and 2 (third and fourth reaction).

It should be emphasized that the transfer of polarization from one radical to another is the result of supramolecular interactions, that is, noncovalent interactions between reactive species. Thus, the TREPR technique is an excellent tool for examining such supramolecular interactions.

2.5. Polarization Sorting—TREPR Evidence for Nonreactive Collisions of Free Radicals: The Radical Pair Mechanism of ESP

A second mechanism exists for the dynamic radical pair (Scheme 2) to produce ESP in nonreactive encounters and collisions of radicals and thus serves as a second probe of supramolecular interactions of radicals with one another. The ESP arises during the dynamic radical pair lifetime as the result of magnetic interactions between initially nonpolarized pairs of radicals in the presence of an applied magnetic field.[1, 3, 4] The ESP is said to be generated through the radical pair mechanism (RPM) and involves an electron exchange induced mixing of magnetic states during the encounter. Only the mixing of ^1S_o and $^3T_0$ is responsible for the RPM because $^3T_+$ and $^3T_-$ split from $^3T_0$ (large energy gap) as the magnetic field increases in magnitude. Since the rates of interconversion between the triplet sublevels and singlet level depend on the energy gap, these two triplet sublevels are essentially cut off from ISC by the Zeeman interaction.

For carbon-centered radicals, either differences in the *g*-factors of the radicals (Δg) or hyperfine coupling can cause the ^1S_o-$^3T_0$ mixing which leads to spin polarization. The effect of Δg is usually smaller than the hyperfine interactions for organic radicals, so that the latter typically dominate the polarization effects in the RPM. Note that for ^1S_o-$^3T_0$ mixing, the number of up and down spins remains constant in the presence of a strong magnetic field.

During an encounter and separation step of a dynamic geminate radical pair, spins of the two partners of the pair are alternately under the influence of the electron exchange interaction (during collision of the pair) and the hyperfine interaction (when the pair is separated by one or more solvent molecules). When hyperfine interactions are responsible for the mixing it is reasonable to expect that some hyperfine states can enhance the mixing faster than others and that these states will be more populated in the free radicals of the pair when separation occurs. The spin states of the two ^2FR that reencounter are mixtures of ^1S and ^3T states. However, these states polarize as if they were triplets, because the pairs with dominant singlet character react efficiently and are thus removed from the paramagnetic pool and leave behind radical pairs that have dominant triplet character. The current theory of polarization of free radicals requires that a pair must first encounter, then separate to a distance for which the value of *J* is near zero, and then return to form a colliding pair.[1, 3, 4] This polarization selection occurs upon radical reencounter under the influence of *J*. The creation of ESP through the RPM depends upon the subsequent action of the electron-exchange interaction *J*, which introduces a "phase shift" into the pair wave function and accumulates more α spin in one radical and more β spin in the other radical. Both ^1S and $^3T_0$ contain equal amounts of α and β spins (vector description of S and T in Scheme 4 bottom), so that mixing cannot create any excess of up or down spins, and any excess of α spins must be balanced by an excess of β spins. Experimentally, the mixing of some hyperfine states of the radicals usually exhibits an excess of absorption (A); other hyperfine states exhibit an emission (E).

The typical result for radicals of the type $^2ACO^{\#}$ and $^2B^{\#}$ of the exemplar is usually (assuming the usual negative sign of the exchange interaction, which means that S has a lower energy than T) the production of a RPM-polarized spectrum in which the line(s) at low field (lower field than *g*) of a doublet are in emission and the high field line(s) (higher field than *g*) are in enhanced absorption. When a spectrum has these characteristics it is said to exhibit an E/A polarization pattern. The energy level diagram that produces such polarization by RPM is shown schematically in Scheme 10 for one of the radicals of the pair. In this example, it is assumed that

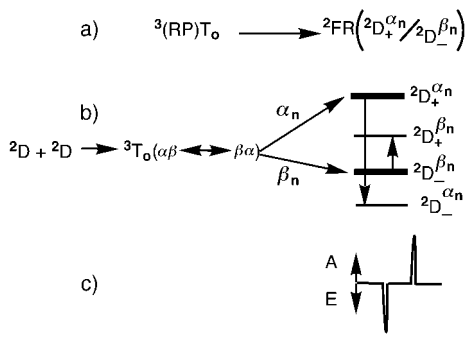

Scheme 10. Schematic energy level diagram for the RPM for polarization. In the case shown, the energy levels are not to scale, J is negative, and the hfc constant is positive. a) A ^{3}RP that diffuses away from each other to yield two ^{2}FR; b) energy level diagram—for simplicity, only one radical coupled to a single spin ½ nucleus is illustrated; c) typical TREPR spectrum derived from the RPM including enhanced emission and an enhanced absorption (E/A) pattern for one of the radicals.

during the mixing the $^2D_-$ state, which is hyperfine coupled to the β_n nuclear spin, is overpopulated and the $^2D_+$ state, which is coupled to the α_n nuclear spin, is also overpopulated. From the energy level diagram it can be seen that such overpopulations lead to an emissive (E) allowed transition from the $^2D_+{}^{\alpha}$ level and an enhanced absorption (A) allowed transition from the $^2D_-{}^{\beta}$ level. The higher energy $^2D_+{}^{\alpha}$ transition occurs at a lower magnetic field in a TREPR experiment.

It is important to keep in mind that the net polarization of the radical ensemble is zero, that is, the number of $\alpha(\uparrow)$ and $\beta(\downarrow)$ spins remains identical to that of the Boltzmann distribution so that the integrated intensity of the RPM to the spectrum is zero before spin relaxation. However, the radicals are polarized far away from the Boltzmann distribution, and the system can be examined by TREPR.

The timescale of production of polarization by the RPM is usually longer than the that by TM, which is expected to be of the order of nanoseconds and is limited by the rate of α-cleavage. The development of RPM polarization requires separation of a radical pair followed by diffusive escape and subsequent encounters. Experimentally, the timescale for the build-up of RPM polarization in carbon-centered radicals is of the order of 100 – 1000 μs.[29]

As an example of the RPM, we consider the photolysis of **2**. The ESP-TREPR spectrum 0.1 – 0.2 μs after laser excitation (Figure 5a) is in total enhanced absorption, whereas at 2 – 5 μs after excitation (Figure 5b) the spectrum transforms into an E/A pattern. This arises from the RPM, which occurs at longer times because of the requirement of separation and reencounters. This is a nice example showing that if α-cleavage is fast enough the TM determines the observed TREPR at short times, but at longer times polarization by the RPM comes into play. We note that in this case the TREPR method allows direct investigation of steps 3 and 4 – 6 of the dynamic radical pair of Scheme 6.

An important feature of RPM is that it represents a spin reorganization among the magnetic sublevels—not a spin creation as occurs in $^1S_1 \rightarrow {}^3T_1$ intersystem crossing nor a spin transfer as occurs in reactive and nonreactive interactions

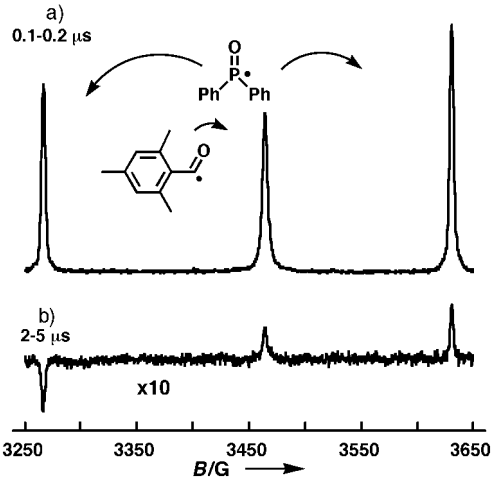

Figure 5. ESP-TREPR spectrum of diphenyl(2,4,6-trimethylbenzoyl)-phosphane oxide (**2**) in ethyl acetate at two times after the laser pulse. The lines at highest and lowest fields are derived from the phosphorus radical, whereas the central line results from trimethylbenzoyl radical.

between radicals. Another important feature is that the RPM depends on the effects of an external field on the spin dynamics of the radical pair. The RPM is more general than the TM in that it does not require the formation of a triplet (free radical encounters which produce ^{3}RP are sufficient) and does not depend on the triplet spin lattice relaxation time. The photolysis of phenyl (*tert*-butyl)phenylketone provides an interesting example for which no TM polarization is observed by TREPR spectroscopy,[30] presumably because in this case the α-cleavage is so slow (ca. 10^7 s^{-1})[17] that equilibration of the triplet sublevels occurs before cleavage and the primary radicals are unpolarized. However, the unpolarized radicals separate and, upon reencountering, produce the expected RPM E/A polarization.

3. Supramolecular Chemistry and Supramolecular Photochemistry

Supramolecular chemistry refers to the structures, dynamics, and transformations of molecules that are "connected" by intermolecular interactions and intermolecular noncovalent "bonds".[31, 32]. Many supramolecular systems may be characterized as guest@host systems for which a small "guest" molecule is adsorbed and noncovalently bonded to a large "host" molecular or aggregate of small molecules. While many of the properties of the guest and host molecules remain intact in the supramolecular system, the guest@host system will have properties that can be ascribed to more than just the sum of its parts.[33] Supramolecular photochemistry is concerned with the effect of absorption of light on supramolecular systems. One of the key questions deals with the empirical criteria for a guest@host system such that it can be usefully termed a supramolecular system. After the molecular properties of a system have been defined theoretically or experimentally, a system is most readily classified as supramolecular when the system exhibits measured properties that are measurably different from the "sum" of the molecular components.[34]

3.1. Supramolecular Spin Chemistry

Let us examine this question of supramolecularity in the framework of the paradigm of Scheme 2 by focusing on the entities ^{3}RP (or ^{1}RP) and ^{2}FR+^{2}FR. We can describe ^{3}RP (or ^{1}RP) as a "supramolecular" entity as the result of its noncovalent intermolecular spin characteristics and interactions. These interactions are missing in free radicals. How do we examine this supramolecular aspect of ^{3}RP (or ^{1}RP) experimentally? An essential difference between ^{3}RP and ^{2}FR+^{2}FR is the intermolecular noncovalent electron exchange interaction J, which causes the electron spins to be correlated, that is, ^{3}RP and ^{1}RP are spin-correlated radical pairs that possess a finite value of J, whereas ^{2}FR+^{2}FR constitute two spin uncorrelated, separate radicals with no intermolecular interactions and therefore possess $J = 0$. In this example, an important issue is the distance between the two radical centers, since the value of J is expected to decrease exponentially with separation between the radical centers. Most importantly, the molecular nature of the radicals remains unchanged, but the reactivity of both radicals is altered by their separation, since the singlet or triplet character depends on distance. This alteration arises from the noncovalent spin interactions between the radicals when they are in proximity to each other. We can see from this analysis that if the magnitude of the electron exchange interaction between two radicals can be measured, then this measurement would provide one of the most subtle empirical criteria for defining the supramolecularity of a radical pair. Indeed, TREPR spectroscopy is one of the few methods that allows the measurement of J-values for ^{3}RP (^{1}RP is EPR "silent") and consequently allows for the experimental examination of the supramolecular features of this reactive intermediate.

As mentioned above, many supramolecular structures can be described as "guest@host" systems. Of interest to this article are those supramolecular systems for which the host may be described as a liquid supramolecular "cage" for a guest. In particular, we are concerned with systems for which ^{3}RP is the guest. Such a system is described as ^{3}RP@cage, which implies that we are concerned with situations involving a spin-correlated radical pair in a liquid cage. We now make a brief excursion to discuss the concept of liquid cages because the concepts are analogous to those describing supramolecular cages.

3.1.1. The Cage Effect—From the Gas Phase to the Molecular Solvent Cage to the Supramolecular Cage

In a seminal paper Franck and Rabinowitch coined the term "cage effect", to make a distinction between features of a photochemical cleavage reaction in the gas phase and those in liquids.[35] The absorption of a photon was considered to excite a molecule to a "dissociative" energy surface (Figure 6). The dissociative surface was considered to be repulsive so that some critical bond of the molecule begins to stretch and then break to produce two radicals (indicated by arrows in Figure 6, top). In the gas phase there are no forces to constrain the radical fragments (no solvent "walls" to contain the radicals), therefore the radical pair dissociates efficiently into two free radicals. However, when a pair of reactive radicals are formed by such a bond cleavage in an inert liquid, the solvent molecules serve as a "cage" around the geminate ("born together") radical pair (Figure 6, bottom). The authors suggested that the probability of escape of a reactive pair of fragments produced by photodissociation is lower in solution compared to the gas phase because of the action of the solvent cage about the pair. The solvent is expected to remove energy and serve as a hindrance or "solvent wall" to separation. Both features will enhance the probability of the recombination. The enhancement in the probability of recombination of a pair of radicals produced by dissociation in a liquid compared to in the gas phase has been termed the "cage" effect produced by solvent molecules in a liquid. However, the solvent walls in a liquid are not impermeable to the radicals, but rather are more or less "porous". The "cage effect", or the probability of recombination of the geminate pairs, will depend on the porosity of the solvent walls.

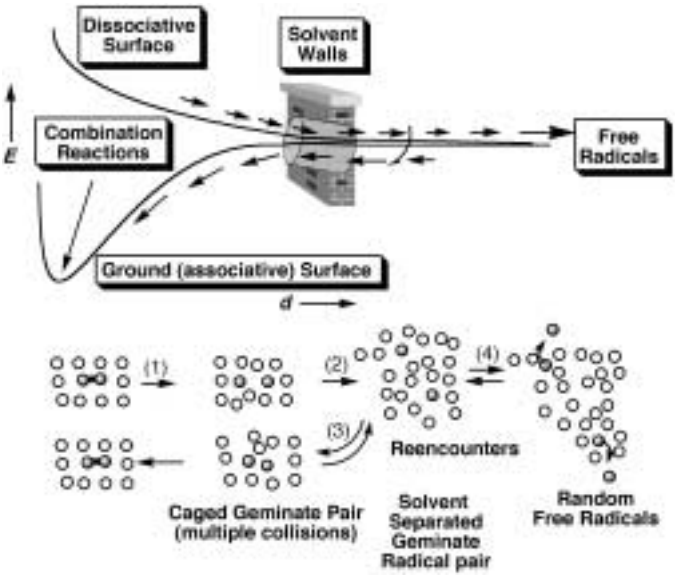

Figure 6. Energy surface and mechanical description of the cage effect. The lower energy curve represents an attractive, ground-state molecule. This molecule is photochemically excited to the dissociative state. As the distance d between the two radical centers increases, the relative energy decreases. At some point, the ^{3}RP may cross over to the ground state (^{1}RP) surface and ultimately recombine. The solvent walls may prevent complete separation and encourage multiple collisions. If the radicals diffuse beyond the initial solvent cage, ^{2}FR+^{2}FR are formed. See text for further discussion.

In a second seminal paper on the cage effect, Rabinowitch and Wood simulated the cage effect in liquids by measuring the behavior of a mechanical container consisting of a series of agitated balls and a control button which was constantly being struck by the balls. Only certain balls were made of conducting material and "collisional hits" were observed from these balls.[36] The "collisions" of molecules in a solvent were "simulated" by this mechanical device. From this device the authors concluded that collisions between molecules that are nearest neighbors in a solvent cage occur in sets.

In a third seminal paper on the cage effect, Noyes pointed out that purely from random walk statistics, the very fact that

a pair of radicals is "born" together in a solvent cage provides them with a certain probability of geminate reaction even after the geminate pair has left the primary solvent cage.[37] Noyes suggested that random diffusive displacement of the pair in the primary cage will be followed by a "reencounter" of the geminate pair in a secondary solvent cage. At this point, there is a certain probability of reaction between the secondary geminate pairs. The Noyes model suggests that the definition of a solvent cage is a region of space in a homogeneous liquid for which the probability of recombination reactions of a geminate radical pair is much higher than the probability of reaction with radicals of pairs generated from other dissociations or with scavengers.

The ideas of these seminal papers are summarized schematically at the bottom of Figure 6. The cleavage of a bond leads to the geminate radical pair in the solvent cage (step 1). The geminate pair undergoes multiple collisions before one or more solvent molecules separates the pair (step 2). The separated pair then either undergoes a reencounter to reform a caged pair (step 3, rare in homogeneous nonviscous liquids) or continues to separate to become free radicals (step 4) that undergo combination reactions with other free radicals generated from separate dissociations. The cage effect is also described, and it is of interest to compare it to the "dynamic radical pair" described in Scheme 2.

3.1.2. The Role of Spin on the Cage Effect—The Molecular Versus the Supramolecular Cage

We now reconsider the idea of the cage effect in terms of a modern paradigm of supramolecular photochemistry which includes the spin of the radicals produced by a photochemical dissociation. We shall show how TREPR spectroscopy can assist in investigating the properties of a triplet geminate radical pair existing in a molecular or a supramolecular cage. Figure 7 expands on the classical ideas of the solvent cage shown in Figure 6 and attempts to show the interrelationships

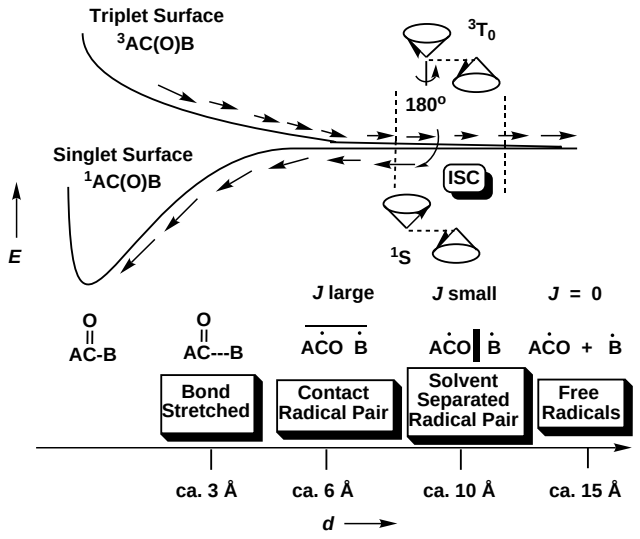

Figure 7. Energy surface description of the cage effect with supramolecular aspects and spin aspects included. The strong electron exchange interaction occurs when the radicals are in close proximity. See text for further discussion.

of electronic energy surfaces, spin interconversions, and the supramolecular cage effect.

In Figure 7 the stereochemistry of the electron spin structure is represented in terms of a conventional vector notation (compare with Scheme 4, bottom). In this notation the two spin vectors are strongly coupled (strong electron exchange interaction, large J-value) when the radical pair is in a collision complex, and the spin vectors are weakly coupled (small J-value) when the radical pair is separated by one or more solvent molecules. When the pair is separated by several solvent molecules, $J = 0$ and the probability of reencounter of the geminate pair in a nonviscous homogeneous solution is also equal to 0, that is, the pair is no longer a geminate pair possessing spin correlation, but a spin uncorrelated pair of free radicals.

When the geminate pair is in a collision complex (termed a contact pair), the exchange interaction is so large that the configuration of the spins is retained during collisions. This result implies that ISC is unlikely to occur in a collision complex because the exchange force for maintaining spin stereochemistry is much more powerful than any available magnetic forces capable of reorienting the spin stereochemistry. However, when the pair has separated in space to several angstroms, the exchange interaction decreases to a value that is small compared to the weak, but available, magnetic interactions, such that the stereochemistry of the spins $^3T_0$ and ^1S_o can be "mixed". Thus, for a recombination reaction to occur starting from a primary triplet geminate pair, the inert triplet geminate pair must separate from a collision complex, singlet character must be introduced, and the pair must reencounter to form a reactive collision complex with singlet character.

In ordinary nonviscous organic solvents the probability of a geminate pair reencountering is statistically very small. Most of the geminate pairs never reencounter and free radicals are formed (compare with the molecular photochemistry paradigm in Scheme 2). A supramolecular liquid environment may be considered as one for which reencounters are enhanced by the "reflecting" walls of a supramolecular boundary (shown schematically as a porous physical wall in Figure 6 and as dashed lines in Figure 7). In the same way that the walls of a solvent cage "reflect" a primary geminate pair into multiple collisions before exiting from the solvent cage, the walls of a supramolecular cage "reflect" a geminate pair into multiple reencounters before allowing exit from the supramolecular cage. However, the important point is that, compared to homogeneous solutions, the supramolecular wall can be much more effective in reflecting radicals back into reencounters and collision complexes. The size of the supercage as well as the chemical characteristics of the solvent walls and of the guest radicals will all be factors in determining the cage effect and radical–radical interactions. Furthermore, the size of the supramolecular cage can be varied, which implies that the distance at which the radicals can separate can also be varied experimentally. Since J depends on the separation of the radicals, J will vary with the size of the supramolecular cage. In Section 3.4.1 we will consider micelles as models of supramolecular cages for radical pairs. However, first we need to consider the influence of J and the supramolecular

interactions of a radical pair in a supercage on the ESP-TREPR spectrum.

3.2. TREPR of Spin-Correlated Radical Pairs—Investigation of the Intermolecular Exchange Interaction

In the paradigm of Scheme 2 the entity ^{3}RP, a spin-correlated triplet geminate radical pair, was considered as a paramagnetic entity and a reactive intermediate that was required to be produced by spin-selection rules as the result of a primary photochemical process from a triplet excited state. We may now ask if TREPR spectroscopy can provide experimental evidence for the existence of such an entity. The lifetime of ^{3}RP (the lifetime of a radical pair in a solvent cage) in homogeneous solutions is less than a nanosecond, which is shorter than the time resolution of the TREPR method. However, the lifetime of ^{3}RP in a supramolecular cage (for example, a micelle) can be manipulated systematically, for example, by changing the size or nature of the supercage. In this manner, the residence time of the pair in a supramolecular cage can be varied from nanoseconds to milliseconds. The direct investigation ^{3}RP within the time resolution of the TREPR technique thus becomes possible by incorporating the pair in a supramolecular cage. From these considerations, we conclude that it should be possible to employ the TREPR technique to investigate geminate radical pairs if the pairs are spin polarized. We now present an analysis of a polarization mechanism that is characteristic for spin-correlated radical pairs, and which allows a TREPR characterization of these species and so definitively allow them to be differentiated from polarized free radicals.[38, 39]

3.3. Magnetic Level Diagram for a Spin-Correlated Radical Pair

Scheme 11 shows a qualitative, schematic description of the magnetic energy diagram for a spin-correlated radical pair (in a solvent cage or a supramolecular cage). We shall use a concrete model as an example of how the spectrum of ^{3}RP

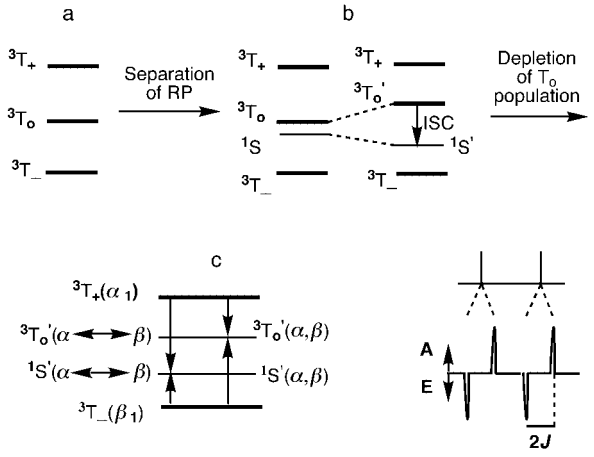

Scheme 11. Schematic energy level diagram of a spin-correlated radical pair and the mechanism of ESP of such a pair. See text for discussion.

becomes polarized in a very interesting manner and how the measurement of a ESP-TREPR spectrum provides information on the average value of the exchange interaction between the radicals. In the model it is assumed that the $^3T_1 \rightarrow {}^3$RP process (step 3 of Scheme 6) leads to equal population (indicated by identical thickness of the levels in Scheme 11a) of all three triplet sublevels, $^3T_+$, $^3T_0$, and $^3T_-$. Further, this model implies that the TM is absent. Again using the exemplar of α-cleavage, the radicals are in close contact immediately after cleavage so that the value of J is high. Under these conditions the $^3T_0$ state is split in energy from the other two triplet levels and ^{1}S is split very far from any of the T levels (the S state is not shown in Scheme 11a because of the large energy separation from the T levels under these conditions).

However, as the radical pair separates in the cage or supercage, the value of J decreases (Figure 7). We consider specifically the situations for which J is of the order of the energy gap between the triplet sublevels, that is, the energy of ^{1}S is lower than that of $^3T_0$ but higher than that of $^3T_-$ (Scheme 11b). Because of their proximity, the $^3T_0$-^{1}S states begin to mix, and as a result the $^3T_0$ level will be selectively depleted as ISC occurs and ^{1}RP are formed and removed rapidly by reaction (Scheme 11b). However, $^3T_+$ and $^3T_-$ do not mix efficiently with ^{1}S because they are energetically separated in energy. The net effect is that $^3T_+$ and $^3T_-$ become overpopulated (spin polarized) relative to $^3T_0$ (shown schematically in Scheme 11c as the thinner lines for the energy levels for the $^3T_0$ and ^{1}S state). Thus, if an EPR spectrum of the radical pair is taken before spin relaxation, an emissive spectrum will occur from transitions from $^3T_+$ (Scheme 11c, α_1 transitions) and an enhanced absorption spectrum (Scheme 11c, β_1 transitions) will occur as the result of transitions from $^3T_-$.

Since mixing between $^3T_0$ and ^{1}S occurs, each state is no longer pure singlet or pure triplet and must be classified as "mixed" states $^3T_0'$ and $^1S'$. As a result, transitions occur from $^3T_+$ and $^3T_-$ to both $^3T_0'$ and $^1S'$ (Scheme 11c). The net result is two emissive transitions $[^3T_+(\alpha_1) \rightarrow {}^3T_0'(\alpha,\beta)$ and $^3T_+(\alpha_1) \rightarrow {}^1S'(\alpha,\beta)]$ and two absorptive transitions $[^3T_-(\beta_1) \rightarrow {}^3T_0'(\alpha,\beta)$ and $^3T_-(\beta) \rightarrow {}^1S'(\alpha,\beta)]$. From this simplified model the experimental ESP-TREPR spectrum will appear as shown in Scheme 11c. Note the remarkable and very characteristic feature predicted by the analysis: each hyperfine component of the polarized spectrum, which normally would be a single line, is observed as an E/A doublet split by 2J. The analysis suggests that if an ESP-TREPR spectrum can be observed the value of the supramolecular interactions, as estimated by J, can be extracted directly from the separation of the E/A doublets in the spectrum. It is worthwhile noting that this analysis holds true in cases where the linewidth of the peak is smaller than the splitting (that is, when the EPR lines are sharp compared to a broad splitting).

For the purposes of this account the main conclusions of the analysis of the energy diagram are the expectation that ^{3}RP in contrast to ^{2}FR will possess hyperfine components that are E/A and that the energy difference corresponding to the separation of the E/A lines will be related to the exchange

interaction. We now describe the properties of micelles that make them excellent models for supramolecular cages for radical pairs and present some experimental examples of ESP-TREPR spectra of ^{3}RP produced in micelles by photochemical α-cleavage of ketones.

3.4. A Structural Model of Micelles—Micelles as Supramolecular Cages

Micelles are self-assemblies that have lifetimes in the vicinity of milliseconds and monomer exchange in the microsecond time domain. Micelles are commonly formed in aqueous solutions from surfactants that have a hydrocarbon chain and a hydrophilic headgroup.[40] The headgroup can be cationic, anionic or non-ionic (Scheme 12). The surfactants aggregate as a result of the hydrophobic effect in such a way

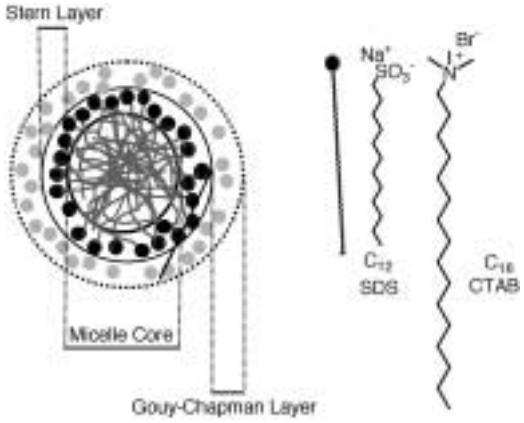

Scheme 12. Left: Schematic representation of a micelle. The black circle represents the ionic portion of the headgroup (for example, SO_3^-), while the long tail depicts the hydrophobic, alkyl chain. Right: Sodium dodecyl sulfate (SDS, C_{12}) and cetyltrimethylammonium bromide (CTAB, C_{16}) each have about 60 monomer units per micelle and are typical anionic and cationic micelle-forming surfactants, respectively.

that the hydrocarbon portions of the surfactant structure avoid water by forming a hydrophobic core consisting of entangled hydrocarbon chains. While the core of the micelle is "oily" and will solubilize organic guests, a certain amount of water penetration is expected.[41] This is an important consideration, because if one is trying to characterize a geminate pair in a micelle by TREPR spectroscopy, observation of the radical species may be occurring on a timescale where monomer exchange, or even complete dissolution of the self-assembly has occurred. ESP-TREPR spectra can be monitored on a nanosecond to microsecond timescale and thus provides an excellent method to observe the dynamics of the radical species within the micelle. On average, micelles are nonspherical and their shape can be modified with a change in the ionic strength, temperature, and pH value. These systemic properties can be changed with ease, so it is quite possible to investigate the transfer of electron spin polarization under a variety of micellar conditions and hence different levels of environmental constraint.

The supramolecular aspects of micelles enable us to divide the host into several potential binding sites (see Scheme 12). The Gouy–Chapman layer is the region in which the anions reside in a solution of sodium dodecyl sulfate (SDS). In this region, it is feasible for a cationic guest to bind to the anionic headgroup. A second binding site may be envisioned in the region between the headgroups (Stern layer), which is fairly polar, and is accessible to the bulk water. Yet another binding site can be the hydrophobic "core" inside the micelles, where one expects guest hydrocarbons and aromatic compounds to be located as a result of the hydrophobic effect. The constraints and diffusional dynamics imposed on molecules in these various micellar regions is one of particular importance in supramolecular chemistry, and to ESP. For example, guest radical pairs will have decreased ability to form free radicals as a consequence of an increased propensity for recombination because of the presence of the supercage. We will now show that the combination of electron polarization and the TREPR technique can be exploited to investigate weak intermolecular interactions, such as the electron exchange responsible for ESPT, between radicals in supramolecular systems.

According to the paradigm, a primary photochemical reaction such as α-cleavage of a triplet ketone ^{3}AC(O)B (Scheme 6), produces a geminate spin correlated radical pair ^{3}(ACO$^\bullet$ $^\bullet$B) inside the solvent cage. The solvent cage has a lifetime of the order of picoseconds for common nonviscous solvents. This lifetime is far too short to be measured directly by the TREPR technique. However, incorporation within a micelle enhances the lifetime of the geminate pair within the micellar supercage by several orders of magnitude.[29, 42–44] The radical pair as a guest and the "supercage" as a host (^{3}RP@supercage) form a long-lived supramolecular structure capable of direct detection by the TREPR technique. We can now move to a discussion of the use of ESP-TREPR studies to characterize a micellar supramolecular assembly.

3.4.1. TREPR of ^{3}RP in Micelles—Models of Supramolecular Systems

We now examine the TREPR spectra of ^{3}RP produced by photochemical α-cleavage of ketones in micelles. The structural and dynamic properties of a supramolecular structure will depend on the characteristics of both the guest (^{3}RP) and host (micelle). Thus, the characteristics of both the micelle structure and the radical pair are expected to determine the features of the TREPR spectra. For example, increased micelle hydrophobicity, or increased micelle size will induce a longer residence time for the RP in the micelle. Low hydrophobicity or small size results in faster exit from the micelle. Thus, the ESP-TREPR spectrum of a ^{3}RP in a small micelle will be similar to that for α-cleavage in homogeneous solution, while a longer lifetime in the micelle will consequently lead to more interaction between the spins and in particular, differences in the exchange interaction will be apparent. In exceptionally large micelles, one could obtain ESP-TREPR spectra similar to those obtained in homogeneous solution because the radicals will be able to separate to a distance where the spins no longer interact. We now consider some experimental examples of the use of TREPR

spectroscopy to examine spin-correlated radical pairs produced in micelles directly.

Scheme 13 shows the TREPR spectrum produced by the photolysis of ketone **3** in an aqueous solution containing *tert*-butanol (top) and in an aqueous solution containing SDS micelles (bottom).[42] The spectrum in homogeneous solution

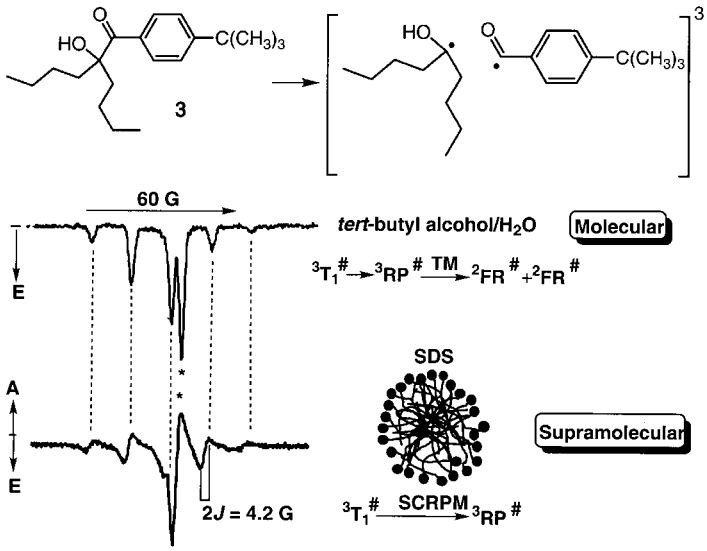

Scheme 13. TREPR spectra obtained 450 – 500 ns after laser flash photolysis of 1.5 mM ketone **3** at 266 nm in a water/*tert*-butyl alcohol (1/1 w/w) mixture and in an aqueous solution of SDS (micelle concentration 1 mM). The signals from the benzoyl radical are marked with an asterisk. The simulation of the supramolecular radical pair is shown in Scheme 15.

(Scheme 13, top) has the appearance of a pair of polarized free radicals whose ESP is produced by the triplet mechanism (compare to Figure 2 a, Section 2.4.1), but in micellar solution, for time scales up to and beyond a microsecond, the spectrum has a very different appearance (Scheme 13, bottom). Each emissive hyperfine line peak in the homogeneous solution spectrum (Scheme 13, top) is matched with a peak that is "split" into E-part at low field and an A-part at high field in the micellar spectrum. This E/A splitting of the hyperfine lines is exactly the spectrum expected for a spin-correlated radical pair ^{3}RP (see Section 3.3 and Scheme 11. Accordingly, in a supramolecular system ^{3}RP@micelle, TREPR spectroscopy provides direct detection and allows characterization of a spin-correlated radical pair ^{3}RP, which is an important intermediate expected from the paradigm.

According to the paradigm the splittings of the hyperfine lines are the result of electron spin – electron spin interactions, so that the separation of these splittings are directly related to the electron exchange interaction J between the partners of the pair in these systems. Thus, from TREPR experiments, one can directly measure the level of intermolecular interactions between two unpaired electrons through measurement of the electron exchange interaction. We will now show that this interaction is a function of supramolecular structure and dynamics of the guest@host system.

3.4.2. TREPR and the Supramolecular Structure of Radical Pairs in Micelles

Let us now consider how TREPR spectroscopy can provide articulation of the paradigm of supramolecular structure of model guest@host systems through a systematic analysis of spin-correlated radical pairs (SCRP) in micelles. The strength of the "bonding" intermolecular interactions responsible for stabilization of the SCRP is expected to depend on both the structure of the components of the pair and on the structure of the micelle. For example, the average proximity of the partners will depend on the micellar size, the hydrophobicity of the core, as well as the size and the hydrophobicity of the partners of the pair. In molecular chemistry, this is akin to the covalent bonding of atoms in a molecule that characteristics of which depend on the component atoms. The magnitude of the electron exchange interaction J depends on the degree of orbital overlap between the two radical centers and consequently the proximity of the partners of the pair. Since the value of J can be extracted from the TREPR spectrum, the technique offers an excellent opportunity to investigate some of the more subtle structural features of a supramolecular system such as SCRP.

As examples of supramolecular structural effects on the radical pair, Scheme 14 shows the TREPR spectra resulting from a systematic investigation of the photolysis of ketone **3** in a series of micelles formed from a series of cationic micelles of alkyltrimethylammonium bromides (C_{10} to C_{16}).[42] The shape

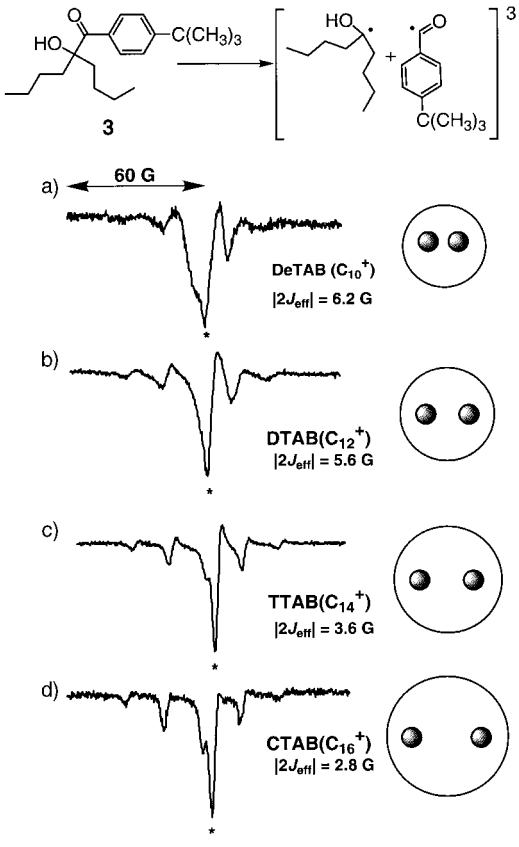

Scheme 14. TREPR spectra obtained during the photolysis of **3** in a series of micellar solutions of alkyltrimethylammonium bromides. The line marked with the asterisk is attributed to the benzoyl radical. For further information see the text.

of the TREPR spectra and the values of J extracted from the spectra show a clear dependence on the alkyl chain length: J drops from 6.2 G for the smallest micelle (C_{10}) to 2.8 G for the largest micelle (C_{16}). In fact, the spectrum for the longest chain (Scheme 14d) is almost purely emissive, with only a small SCRP component. It is worth noting that the lack of the observation of the SCRP mechanism in the case of the largest micelles might be a result of the short lifetime of the radical pair. These same trends were seen using the same hydrophobic precursor of the radical pair placed in anionic micelles formed from a series of alkyl sulfates of different chain length.

The above results demonstrate how ESP-TREPR spectroscopy, through extraction of J-values, can reveal how the size of the micellar host can control the average proximity of the partners of the guest radical pair. Since a radical pair in a micelle is a supramolecular structure, we expect the guest structure will also influence the proximity of the partner and the value of J.

Scheme 15 shows the TREPR spectra of a series of radical pairs **4a**–**d** of differing structures produced by α-cleavage of related ketones in SDS micelles. The electronic and magnetic properties of each of the pairs are very similar. However a major difference in the characteristics of the pairs in SDS micelles is their supramolecular structure. Assuming that hydrophobicity will be a dominant feature in determining the supramolecular stability of the ^{3}RP@micelle structure, the lifetime of the fragments of the pair is expected to correlate with the number of hydrocarbon fragments in the pair. In the case of pairs **4a** and **4b** the ESP-TREPR spectrum in SDS micelles shows essentially no SCPR component ($J \approx 0$ G) and the spectrum appears analogous to that observed in homogeneous solution (compare to Scheme 13a). However, the TREPR spectra for the pairs **4c** and **4d** show significant SCRP contribution and the values of J extracted from the spectra are 3.8 and 4.2 G, respectively.

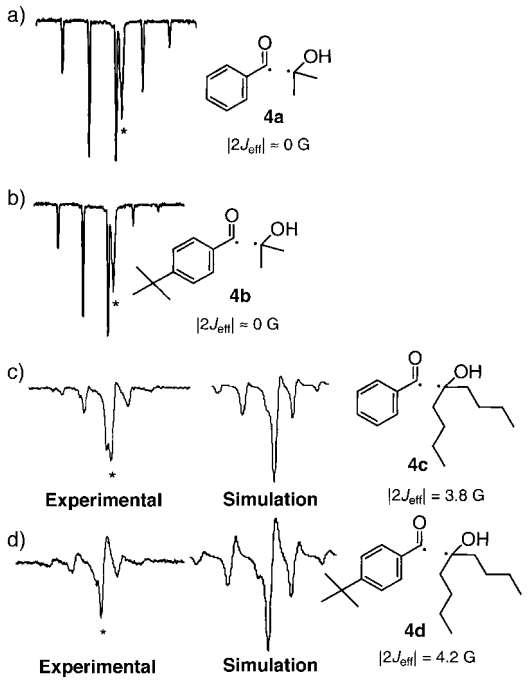

Scheme 15. ESP-TREPR spectra of radical pairs **4a**–**d** in a micellar SDS solution recorded about 500 ns after laser flash excitation. For radical pairs **4a** and **4b** the experimental spectra are shown. Both the experimental and simulated spectra are shown for **4c** and **4d**. The lines attributed to the benzoyl radical are marked with asterisks. The remainder of the spectrum is attributed to the ketyl radical partner of the pair. The experimental spectra can be well simulated and the value of $2J$ is extracted from this process. Note that the value of the electron exchange interaction increases as the relative hydrophobicity (as measured by the number of hydrocarbon fragments) of the pair increases.

It is expected that the hydrophobic character of a radical pair will be important in determining the supramolecular structure and dynamics of the pair in a given micelle. For the radical pairs **4a** and **4b**, both of which consist of one small hydrophilic C_3 ketyl fragment, the rate of escape from the micelle of this small fragment is evidently faster than the time resolution of the TREPR measurement. The ESP-TREPR spectrum observed is essentially the same as that for homogeneous solution (Scheme 15a, b) and the system does not appear to have supramolecular spin properties. However, for radical pairs **4c** and **4d**, which contain two relatively hydrophobic fragments, the residence time of the pair in the micelle is within the time resolution of the TREPR experiment and the ESP-TREPR of SCRP's are observed (Scheme 15c, d). Thus, the supramolecular characteristics of the ^{3}RP@micelle are directly observed. One can observe directly from the experimental results that exit of one of the radical partners from the micelle destroys the "supramolecularity" of the system. In general, the function of the parts is the same as the function of the whole system when only one ^{2}FR is located within the micelle. However, the presence of an exchange interaction when two ^{2}FR are located in the hydrophobic core ensures that the overall reactivity of the system changes. Thus, this experiment clearly demonstrates that spin chemistry, electron interaction, and TREPR spectroscopy can determine the "extent of supramolecularity" of a given system with spin.

The variation in the supramolecular structure of a radical pair in a micelle as a function of supramolecular hydrophobicity is analogous to the "molecular system" of a biradical whose radical centers are separated by flexible covalent linkages. In this case shorter chains result in a greater degree of orbital overlap between the radical centers. In both situations, the exchange interaction is increased by the closer proximity of the radical species. Indeed, the ESP-TREPR spectra of biradicals display the expected dependence of J on the chain length.[11]

4. Other Applications of the TREPR Technique and ESP

A goal of this account is to inform the interested reader that TREPR spectroscopy is a powerful technique for the investigation of paramagnetic species (triplets, radical pairs, free radicals) produced in many photochemical reactions. For the sake of clarity the presentation concentrated on a single exemplar paradigm, the α-cleavage of carbonyl compounds. However, the TREPR technique has been employed to investigate all of the important primary photochemical processes of ketones[5] including those producing biradicals.[2, 11, 38, 39] In addition to the photoreactions of ketones,

many other organic substrates[1–6, 28, 45, 46] have also been investigated by this technique. The TREPR technique and ESP have also been powerful tools for the investigation of problems particularly of interest in the area of photosynthesis, for example, to provide direct evidence for a specific electron acceptor in photosystem I,[47] and elucidation of donor–acceptor pairs in the bacterial photosynthetic reaction center.[48, 53, 54] A recent study in photosynthetic models has revealed structural information using a zinc porphyrin with a *para* arrangement of *N*,*N*,*N*′,*N*′-tetraalkyl-*para*-phenylenediamine and naphthoquinone units.[49] Other studies dealing with the photosynthetic reaction center demonstrate that additional kinetics and structural information can be obtained by operating the EPR spectrometer at various frequencies.[50, 51] The energy and electron-transfer processes of the fractions of the photosynthetic reaction center have been used in the form of liquid crystals.[52] Other groups have used these spin techniques to understand the interaction between electrons at close ranges in processes involving polarized electronic spin within supramolecular systems, such as micelles[55] and cyclodextrins.[56] These are just a few of the examples that demonstrate how important and vital the ESP-TREPR technique and other techniques based on TREPR are in helping to unravel the mystery of how electrons interact with each other and how solar energy gets converted into chemical energy.

5. Summar

This account has attempted to bring together, in a qualitative and conceptual manner, the power of employing TREPR to exploit electron spin polarization (ESP) that is created, transferred, and sorted in many photochemical processes. The ESP that is created serves as a mechanistic tool for the investigation of the paramagnetic species involved in the exemplar paradigm for the α-cleavage reactions of carbonyl compounds and can be examined by TREPR spectroscopy. The exchange interaction is involved in the transfer of spin polarization in nonreactive collisions between triplet radical pairs, in the generation of polarization by the RPM, as well as in the splitting of energy levels leading to polarization and the characteristic transitions of spin-correlated radical pairs. For this reason, geminate triplet radical pairs are excellent models for the investigation of supramolecular noncovalent interactions. The observation of the ESP-TREPR spectrum of triplet radical pairs in supercages such as micelles allows the direct investigation of supramolecular RP@micelle systems in detail through the extraction of *J*-values from the E/A splittings of the hyperfine lines in the TREPR spectra. In fact, it has been shown that the TREPR experiment can directly interrogate spin chemistry and electron interactions. Consequently, the TREPR technique can also determine the "extent of supramolecularity" for a system with spin.

Abbreviations

#	polarized, unpaired electron spin
$\vec{B}_0$	magnetic field
D	doublet electronic state (also free radical, ^{2}FR)
EPR	electron paramagnetic resonance
ESP	electron spin polarization
ESPT	electron spin polarization transfer
^{2}FR	free radical
g_e	*g*-factor (2.0023 for free electron, g_e)
hfc	hyperfine coupling
HOMO	highest occupied (ground state) molecular orbital
I	reactive intermediate
ISC	intersystem crossing
J	electron exchange interaction
k_B	Boltzmann constant
LUMO	lowest unoccupied (ground state) orbital
μ	magnetic moment
P	product
R	reactant
*R	excited state of reactant
RP	radical pair
^{1}RP	singlet radical pair
^{3}RP	triplet radical pair
^{3}RP@cage	Host–guest complex involving a ^{3}RP and a cage host system
RPM	radical pair mechanism
S	spin of an electron
$^1S_0$	ground state singlet
$^1S_1$	excited singlet state
SCRP	spin correlated radical pair
SOMO	singly occupied orbital
SOC	spin–orbit coupling
$^3T_1$	excited triplet state
TM	triplet mechanism
TREPR	time-resolved electron paramagnetic resonance

The authors are grateful to the NSF and the Camille and Henry Dreyfus Foundation for support. They also acknowledge the important contributions to the development of the TREPR technique at Columbia from Matt Zimmt, William Jenks, Joe Wu, Igor Khudyakov, Igor Koptyug, Valery Tarasov, and Steffen Jockusch. Professors Malcom Forbes, Hanns Fischer, Henning Paul, and Hans VanWilligen are thanked for providing useful insights. Professor Keith McLauchlan is thanked for hosting N.J.T. in his laboratory and educating him in the delights of spin polarization and TREPR. We also acknowledge Rene Williams for providing some unpublished work and helpful discussions.

Received: November 16, 1999
Revised: March 1, 2000 [A 370]

[1] K. McLauchlan, M. T. Yeung in *Electron Spin Resonance*, *Vol. 14*, The Royal Society of Chemistry, Cambridge, **1994**, pp. 33–62.
[2] M. D. E. Forbes, *Photochem. Photobiol.* **1997**, *65*, 73–81.
[3] K. A. McLauchlan, *J. Chem. Soc. Perkin Trans. 2* **1997**, 2465–2472.
[4] K. A. McLauchlan, D. G. Stevens, *Acc. Chem. Res.* **1988**, *21*, 54–59.
[5] J. K. S. Wan, M. C. Depew, *Res. Chem. Intermed.* **1992**, *18*, 227–292.
[6] N. Hirota, S. Yamauchi in *Dynamics of Excited Molecules*, *Vol. 82* (Ed.: K. Kuchitsu), Elsevier, Amsterdam, **1994**, pp. 513–557.
[7] H. van Willigen, P. R. Levstein, M. H. Ebersole, *Chem. Rev.* **1993**, *93*, 173–197.

[8] T. S. Kuhn, *The Structure of Scientific Revolutions*, University of Chicago Press, Chicago, **1970**.
[9] N. J. Turro, M. Garcia-Garibay in *Photochemistry in Organized and Constrained Spaces* (Ed.: V. Ramamurthy), VCH, New York, **1991**, pp. 1 – 38.
[10] C. Doubleday, Jr., N. Turro, J. Wang, *Acc. Chem. Res.* **1989**, *22*, 199 – 205.
[11] G. L. Closs, M. D. E. Forbes, *J. Phys. Chem.* **1991**, *95*, 1924 – 1933.
[12] K. A. McLauchlan, *Magnetic Resonance*, Clarendon Press, Oxford, **1972**.
[13] A. Carington, A. D. McLachlan, *Introduction to Magnetic Resonance*, Harper and Row, New York, **1967**.
[14] N. Bunce, *J. Chem. Educ.* **1987**, *64*, 907 – 914.
[15] A. Kawai, K. Obi, *Res. Chem. Intermed.* **1993**, *19*, 865 – 894.
[16] G. Elger, M. Fuhs, P. Müller, J. von Gersdorff, A. Wiehe, H. Kurreck, K. Möbius, *Mol. Phys.* **1998**, *95*, 1309 – 1323.
[17] N. J. Turro, *Modern Molecular Photochemistry*, Benjamin/Cummings, Menlo Park, USA, **1978**.
[18] A. Gilbert, J. Baggott, *Essentials of Molecular Photochemistry*, CRC, Boca Raton, USA, **1991**.
[19] G.-H. Goudsmit, H. Paul, *Chem. Phys. Lett.* **1996**, *260*, 453 – 457.
[20] J. Fujisawa, Y. Ohba, S. Yamauchi, *Chem. Phys. Lett.* **1998**, *282*, 181 – 186.
[21] J. Fujisawa, Y. Ohba, S. Yamauchi, *J. Am. Chem. Soc.* **1997**, *119*, 8736 – 8737.
[22] M. Mukai, S. Yamauchi, N. Hirota, M. Koyanagi, H. Futami, *Bull. Chem. Soc. Jpn.* **1992**, *65*, 1679 – 1684.
[23] I. V. Koptyug, N. D. Ghatlia, G. W. Sluggett, N. J. Turro, S. Ganapathy, W. G. Bentrude, *J. Am. Chem. Soc.* **1995**, *117*, 9486 – 9491.
[24] E. Karaketin, B. O'Shaughnessy, N. J. Turro, *Macromolecules* **1998**, *31*, 7992 – 7995.
[25] A. L. J. Beckwith, S. Brumby, R. F. Claridge, R. Crocket, E. Roduner, *Radical Reactions Rates in Liquids*, *Vol. 18*, Springer, Berlin, **1994**.
[26] A. Kamachi, A. Kajiwara, K. Saegusa, Y. Morishima, *Macromolecules* **1993**, *26*, 7369 – 7371.
[27] Y. Mizuta, N. Morishita, K. Kuwata, *Chem. Lett.* **1999**, 311 – 312.
[28] W. S. Jenks, N. J. Turro, *J. Am. Chem. Soc.* **1990**, *112*, 9009 – 9011.
[29] C. D. Buckley, D. A. Hunter, P. J. Hore, K. A. McLauchlan, *Chem. Phys. Lett.* **1987**, *135*, 307 – 312.
[30] T. Ikoma, K. Akiyama, S. Tero-Kubota, Y. Ikemgami, *Chem. Lett.* **1990**, 1491 – 1495.
[31] J.-M. Lehn, *Angew. Chem.* **1988**, *100*, 91 – 116; *Angew. Chem. Int. Ed. Engl.* **1988**, *27*, 89 – 112.
[32] *Frontiers in Supramolecular Chemistry and Photochemistry* (Eds.: H.-J. Schneider, H. Dürr), VCH, Weinheim, **1991**.
[33] V. Balzani, F. Scandola, *Supamolecular Photochemistry*, Ellis Horwood, New York, **1991**.
[34] M. H. Kleinman, C. Bohne in *Organic Photochemistry: Molecular and Supramolecular Photochemistry*, *Vol. 1* (Eds.: V. Ramamurthy, K. S. Schanze), Marcel Dekker, New York, **1997**, pp. 391 – 466.
[35] J. Franck, E. Rabinowitsch, *Trans. Faraday Soc.* **1934**, *30*, 120 – 131.
[36] E. Rabinowitch, W. C. Wood, *Trans. Faraday Soc.* **1936**, *32*, 1381 – 1387.
[37] R. M. Noyes, *J. Am. Chem. Soc.* **1955**, *77*, 2042 – 2045.
[38] G. L. Closs, M. D. E. Forbes, J. R. Norris, *J. Phys. Chem.* **1987**, *91*, 3592 – 3599.
[39] M. D. E. Forbes, S. R. Ruberu, K. E. Dukes, *J. Am. Chem. Soc.* **1994**, *116*, 7299 – 7307.
[40] C. Tanford, *The Hydrophobic Effect: Formation of Micelles and Biological Membranes*, Wiley, New York, **1980**.
[41] F. M. Menger, R. Zana, B. Lindman, *J. Chem. Educ.* **1998**, *75*, 115.
[42] C. Wu, W. S. Jenks, I. V. Koptyug, N. D. Ghatlia, M. Lipson, V. Tarasov, N. J. Turro, *J. Am. Chem. Soc.* **1993**, *115*, 9583 – 9595.
[43] A. D. Trifunac, D. J. Nelson, *Chem. Phys. Lett.* **1977**, *46*, 346 – 348.
[44] H. Murai, Y. Sakaguchi, H. Hayashi, Y. J. I'Haya, *J. Phys. Chem.* **1986**, *90*, 113 – 118.
[45] G. R. Eaton, S. S. Eaton, K. M. Salikhov, *Foundations of Modern EPR*, World Scientific Publishing, Singapore, **1998**.
[46] K. M. Salikhov, Y. N. Molin, R. Z. Sagdeev, A. L. Buchachenko, *Spin Polarization and Magnetic Effects in Radical Reactions*, *Vol. 22*, Elsevier, New York, **1984**.
[47] S. W. Snyder, R. R. Rustandi, J. Biggins, J. R. Norris, M. C. Thurnauer, *Proc. Natl. Acad. Sci. USA* **1991**, *88*, 9895 – 9896.
[48] S. W. Snyder, A. L. Morris, S. R. Bondeson, J. R. Norris, M. C. Thurnauer, *J. Am. Chem. Soc.* **1993**, *115*, 3774 – 3775.
[49] A. M. Kiefer, S. M. Kast, M. R. Wasielewski, K. Laukenmann, G. Kothe, *J. Am. Chem. Soc.* **1999**, *121*, 188 – 198.
[50] A. van der Est, C. Hager-Braun, W. Leibl, G. Hauska, D. Stehlik, *Biochim. Biophys. Acta* **1998**, *1409*, 87 – 98.
[51] R. J. Hulsebosch, I. V. Borovykh, S. V. Paschenko, P. Gast, A. J. Hoff, *J. Phys. Chem. B* **1999**, *103*, 6815 – 6823.
[52] H. Levanon, K. Hasharoni, *Prog. React. Kinet.* **1995**, *20*, 309 – 346.
[53] H. Levanon, K. Möbius, *Annu. Rev. Biophys. Biomolec. Struct.* **1997**, *26*, 495 – 540.
[54] D. Stehlik, K. Möbius, *Annu. Rev. Phys. Chem.* **1997**, *48*, 745 – 784.
[55] K. Ohara, Y. Miura, M. Terazima, N. Hirota, *J. Phys. Chem. B* **1997**, *101*, 605 – 611.
[56] Y. Kitahama, H. Murai, *Chem. Phys. Lett.* **1996**, *261*, 160 – 164.